



---

## *Robotics 1*

# Robot components: Exteroceptive sensors

Prof. Alessandro De Luca

DIPARTIMENTO DI INGEGNERIA INFORMATICA  
AUTOMATICA E GESTIONALE ANTONIO RUBERTI





# Summary

---

- force sensors
  - strain gauges and joint torque sensor
  - 6D force/torque (F/T) sensor at robot wrist
  - RCC = Remote Center of Compliance (*not a sensor, but similar...*)
- proximity/distance sensors
  - infrared (IF)
  - ultrasound (US)
  - laser
  - with structured light
- vision
- examples of robot sensor equipments
- some **videos** intertwined, with applications

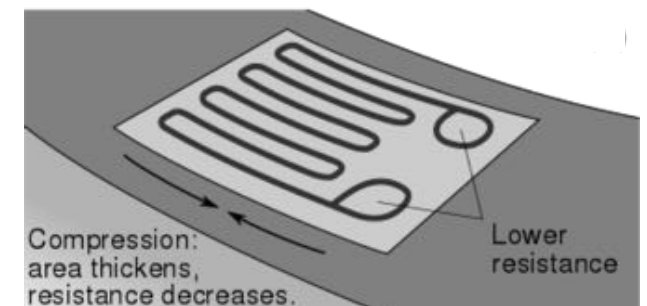
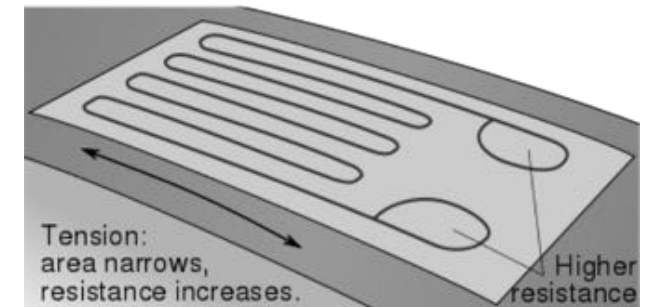
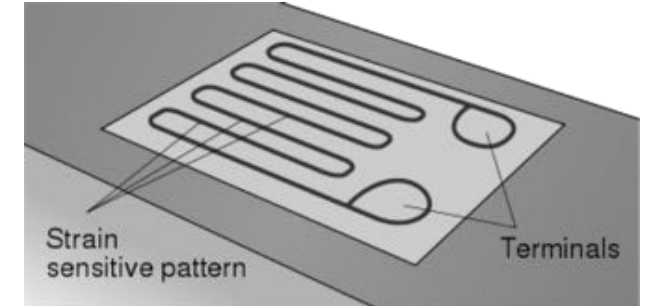


# Force/torque and deformation

- indirect information obtained from the measure of **deformation** of an elastic element subject to the force or torque to be measured
- basic component is a *strain gauge*: uses the variation of the resistance  $R$  of a metal conductor when its length  $L$  or cross-section  $S$  vary

$$\frac{\partial R}{\partial L} > 0 \quad \frac{\partial R}{\partial S} < 0$$

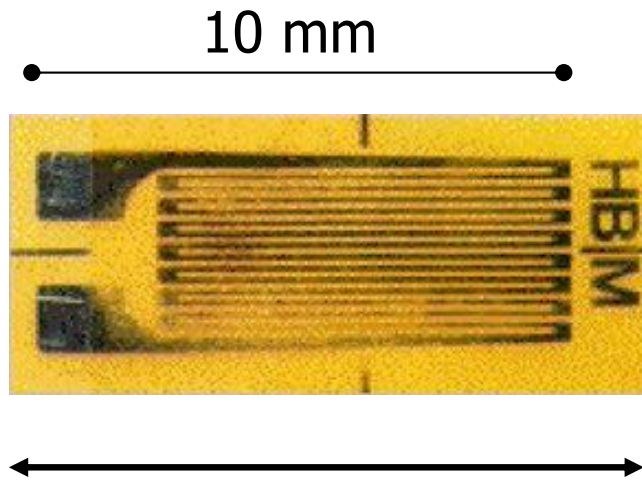
$$\frac{\partial R}{\partial T} \text{ small}$$



temperature



# Strain gauges



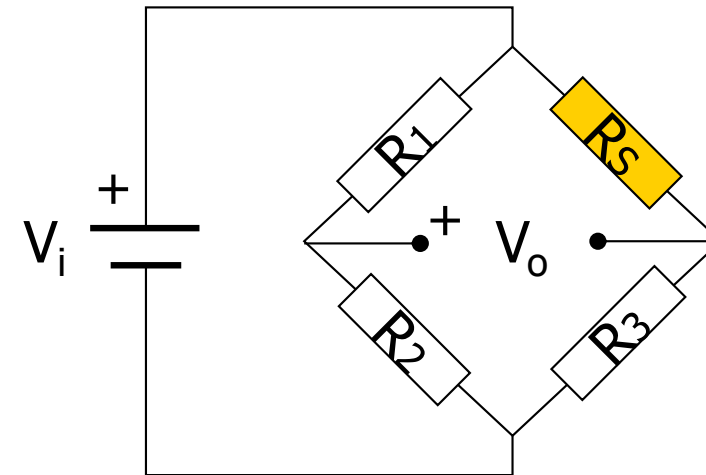
principal measurement axis

$$\text{Gauge-Factor} = GF = \frac{\Delta R/R}{\Delta L/L} \quad \text{strain } \varepsilon$$

(typically GF  $\approx 2$ , i.e., small sensitivity)

if  $R_1$  has the same dependence on T of  $R_S$   
thermal variations are automatically  
compensated

Wheatstone **single-point** bridge connection  
(for *accurately* measuring resistance)



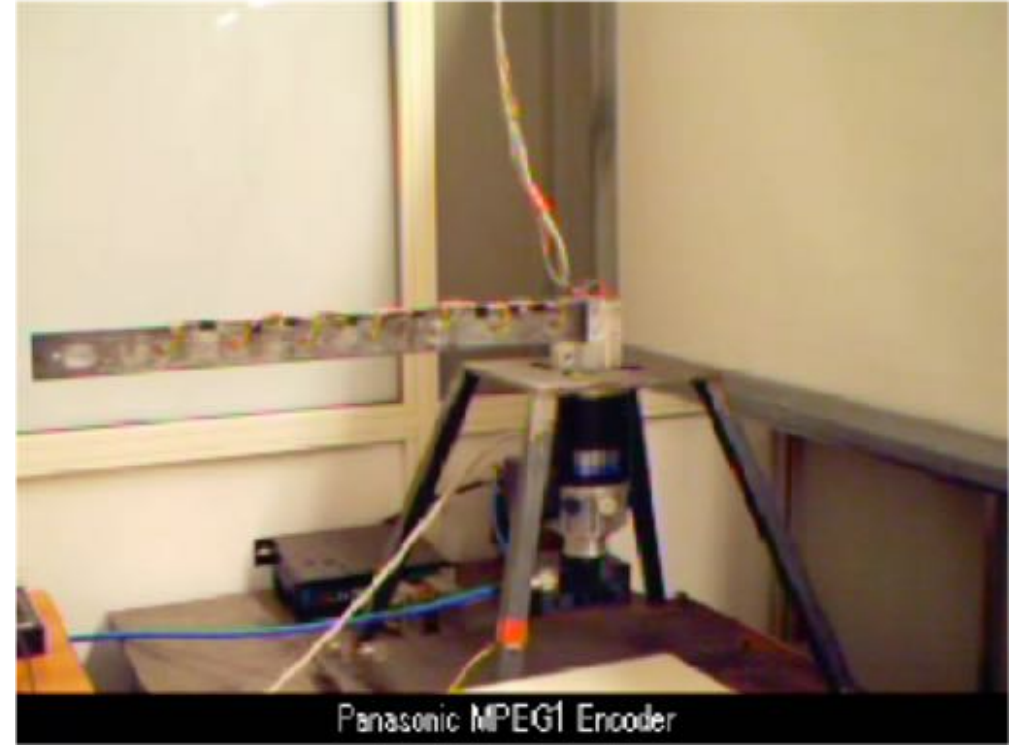
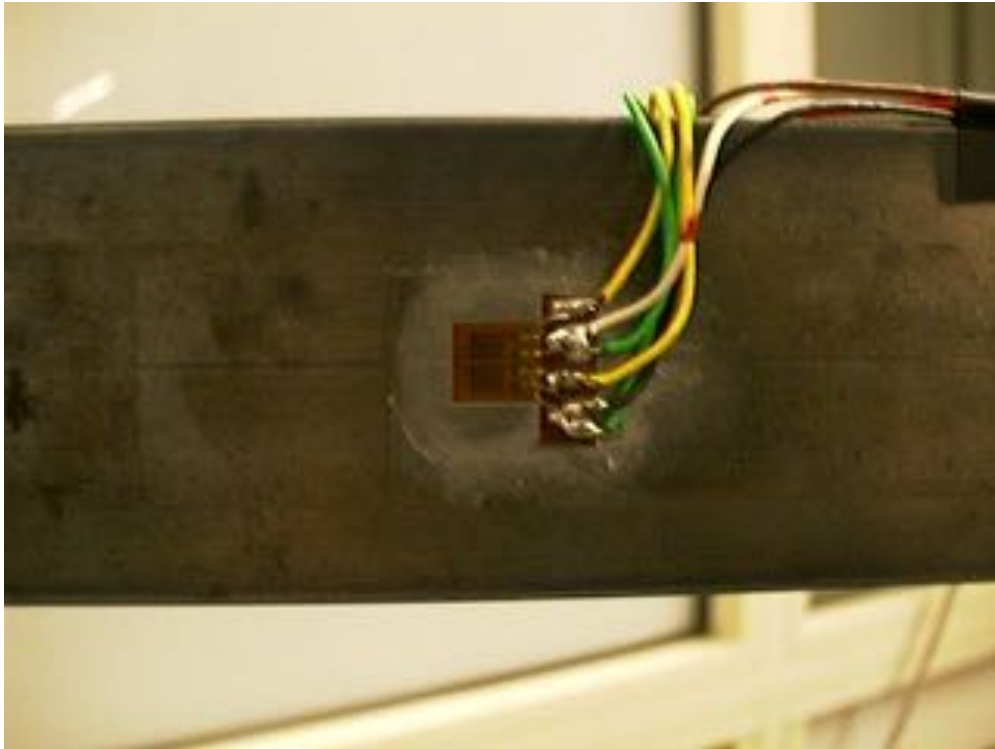
- $R_1$ ,  $R_2$ ,  $R_3$  very well matched ( $\approx R$ )
- $R_S \approx R$  at rest (no stress)
- **two-point** bridges have 2 strain gauges connected oppositely ( $\nearrow$  sensitivity)

$$V_o = \left( \frac{R_2}{R_1+R_2} - \frac{R_3}{R_3+R_S} \right) V_i$$



# Strain gauges in flexible arms

[video](#)

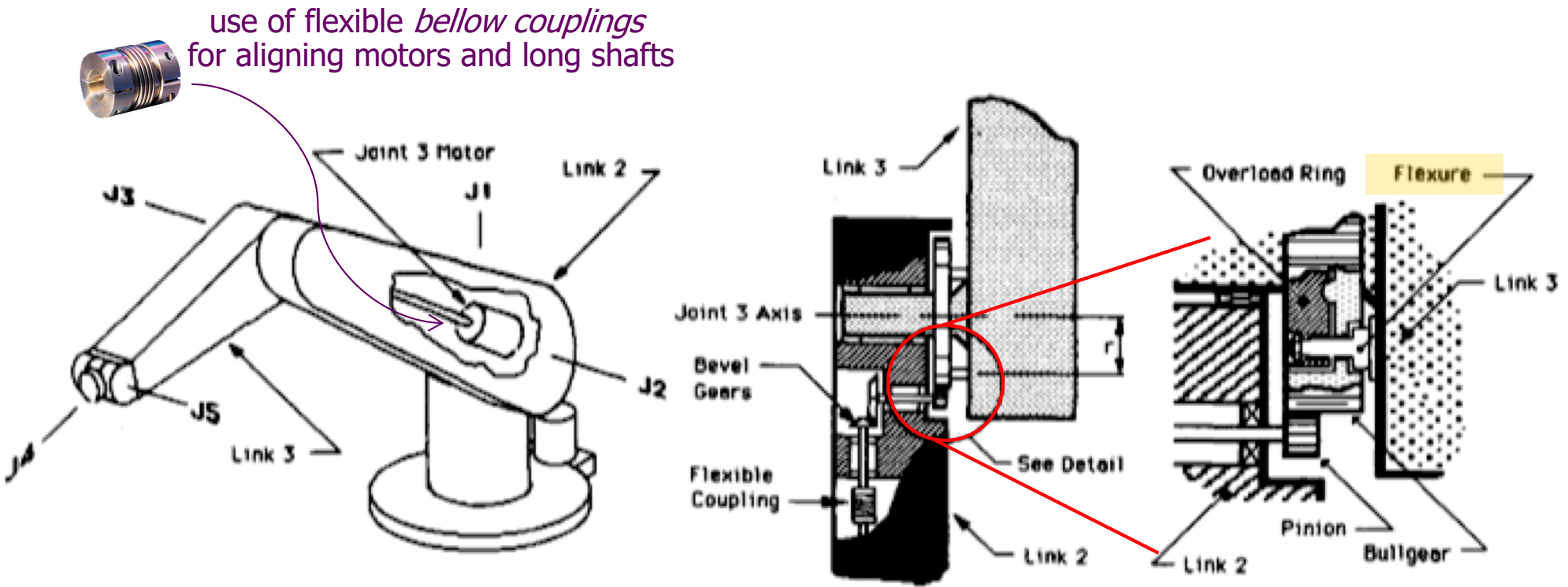


7 strain gauges glued<sup>(1)</sup> to a flexible aluminum beam (a robot “link”) measuring its local “curvature” in dynamic bending during slew motions (a proprioceptive use of these sensors)

<sup>(1)</sup> by cyanoacrylic glue



# Torque sensor at robot joints



strain gauge mounted to “sense” the axial deformation of the transmission shaft of joint #3 (elbow) in a PUMA 500 robot (again, a **proprioceptive** use of this sensor)



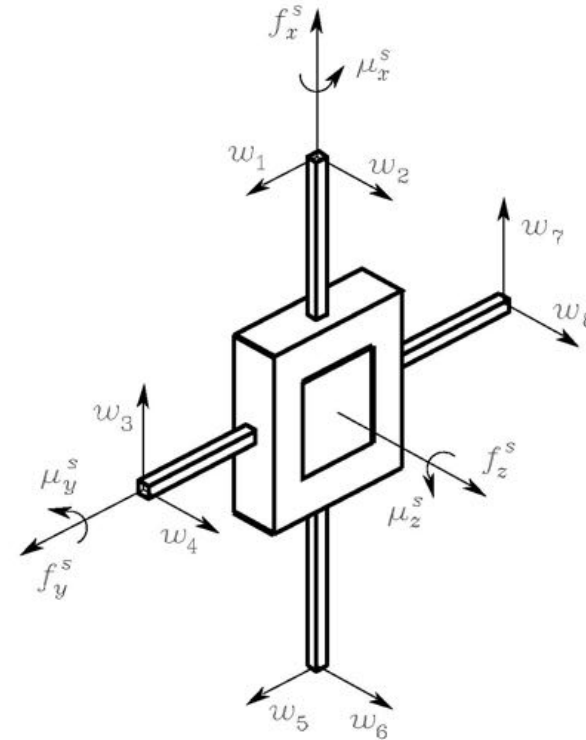
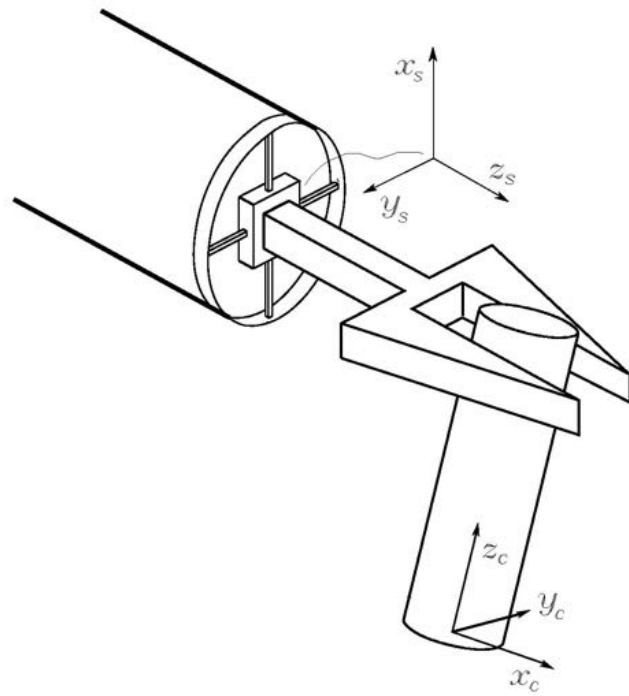
# Force/torque sensor at robot wrist

---

- a device (with the outer form of a cylinder), typically located between the last robot link and its end-effector
- top and bottom plates are mechanically connected by a number of **deformable elements** subject to **strain** under the action of forces and moments
- there should be at least one such element in any direction along/around which a force or torque measure is needed
- since a complete “decoupling” of these measurements is hard to obtain, there are  $N \geq 6$  such deformable elements
- on each element, a **pair of strain gauges** is glued so as to undergo opposite deformations (e.g., traction/compression) along the main axis of measurement



# Maltese-cross configuration



- diameter  $\approx 10$  cm
- height  $\approx 5$  cm
- $50 \div 500$  N (resolution 0.1%)
- $5 \div 70$  Nm (resolution 0.05%)
- sample frequency  $\approx 1$  KHz

- 4 deformable elements
- two pairs of strain gauges are mounted on opposite sides of each element (8 pairs)
- the two gauges of each pair are placed adjacent on the same Wheatstone bridge



# 6D force/torque sensors

- ATI series
- cost (in 2016): about 6 K€ for Mini45 model + 700 € DAQ card

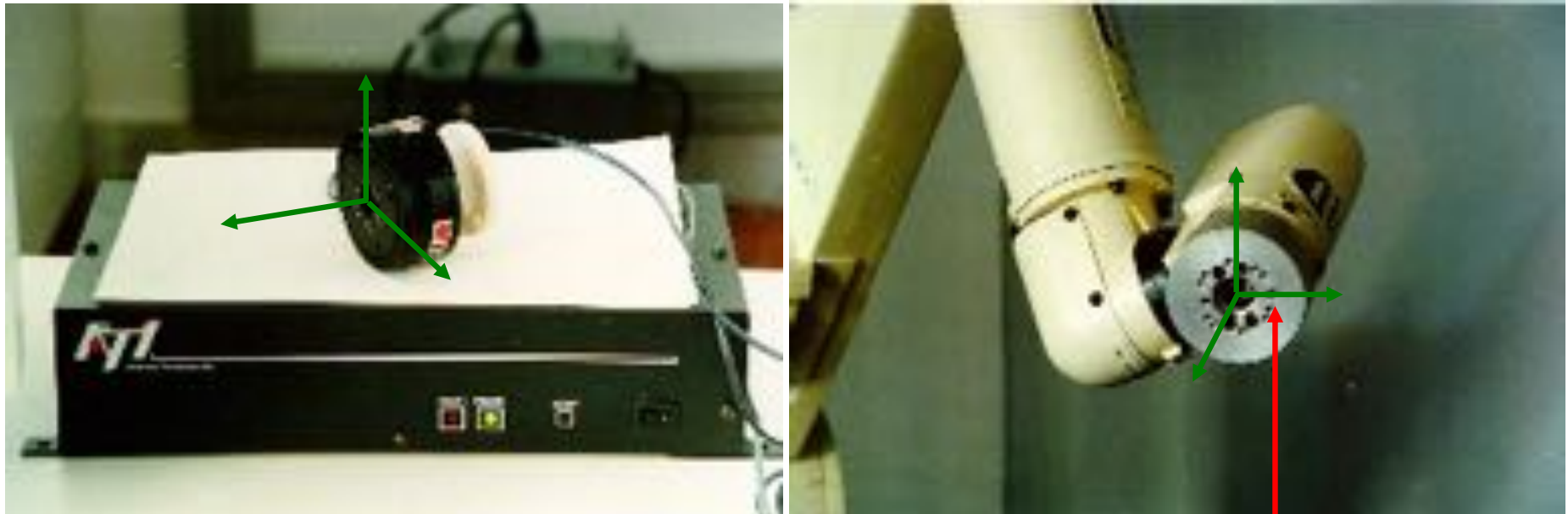


Model	Max Fx,Fy*	Max Tx,Ty*	Weight**	Diameter**	Height**
Nano17	±50 N	±500 N-mm	0.0091 kg	17 mm	14 mm
Nano25	±250 N	±6 N-m	0.064 kg	25 mm	22 mm
Nano43	±36 N	±500 N-mm	0.041 kg	43 mm	11 mm
Mini40	±80 N	±4 N-m	0.05 kg	40 mm	12 mm
Mini45	±580 N	±20 N-m	0.091 kg	45 mm	16 mm
Gamma	±130 N	±10 N-m	0.25 kg	75 mm	33 mm
Delta	±660 N	±60 N-m	0.91 kg	94 mm	33 mm
Theta	±2500 N	±400 N-m	5 kg	150 mm	61 mm
Omega160	±2500 N	±400 N-m	2.7 kg	160 mm	56 mm
Omega190	±7200 N	±1400 N-m	6.4 kg	190 mm	56 mm



# 6D force/torque sensor

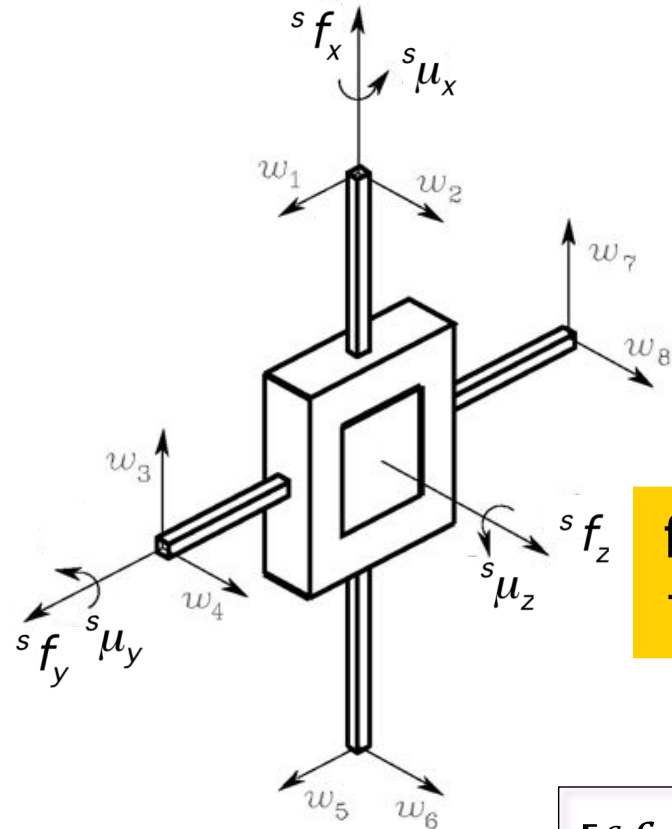
- electronic processing unit and mounting on an industrial robot (Comau Smart 3 robot, 6R kinematics)



mounting flange  
(on link 6 of the manipulator arm)



# 6D F/T sensor calibration



$$\begin{bmatrix} {}^s f_x \\ {}^s f_y \\ {}^s f_z \\ {}^s \mu_x \\ {}^s \mu_y \\ {}^s \mu_z \end{bmatrix} = \begin{bmatrix} 0 & 0 & c_{13} & 0 & 0 & 0 & c_{17} & 0 \\ c_{21} & 0 & 0 & 0 & c_{25} & 0 & 0 & 0 \\ 0 & c_{32} & 0 & c_{34} & 0 & c_{36} & 0 & c_{38} \\ 0 & 0 & 0 & c_{44} & 0 & 0 & 0 & c_{48} \\ 0 & c_{52} & 0 & 0 & 0 & c_{56} & 0 & 0 \\ c_{61} & 0 & c_{63} & 0 & c_{65} & 0 & c_{67} & 0 \end{bmatrix} \begin{bmatrix} w_1 \\ w_2 \\ w_3 \\ w_4 \\ w_5 \\ w_6 \\ w_7 \\ w_8 \end{bmatrix}$$

force/torque measured in the frame attached to the sensor

calibration matrix

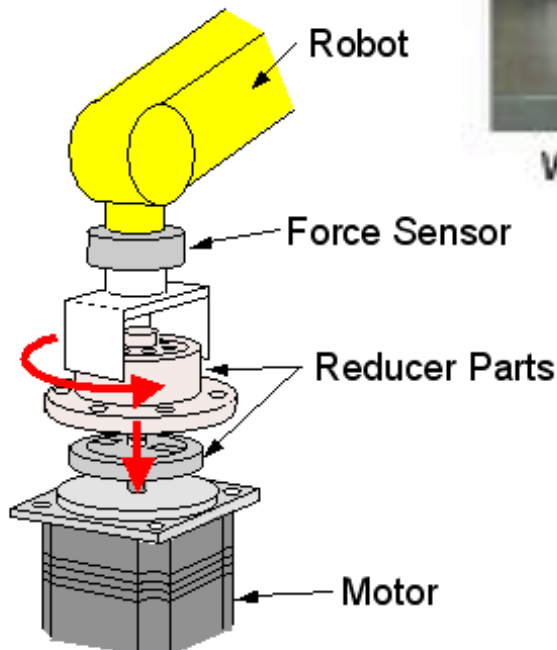
output of Wheatstone bridges

$$\begin{bmatrix} {}^c f_c \\ {}^c \mu_c \end{bmatrix} = \begin{bmatrix} {}^c R_s & 0 \\ S({}^c r_{cs}) {}^c R_s & {}^c R_s \end{bmatrix} \begin{bmatrix} {}^s f_s \\ {}^s \mu_s \end{bmatrix}$$

transformation from the sensor frame to the load/contact frame (at TCP)



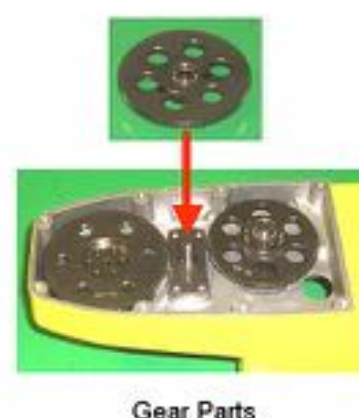
# Typical uses of a F/T sensor



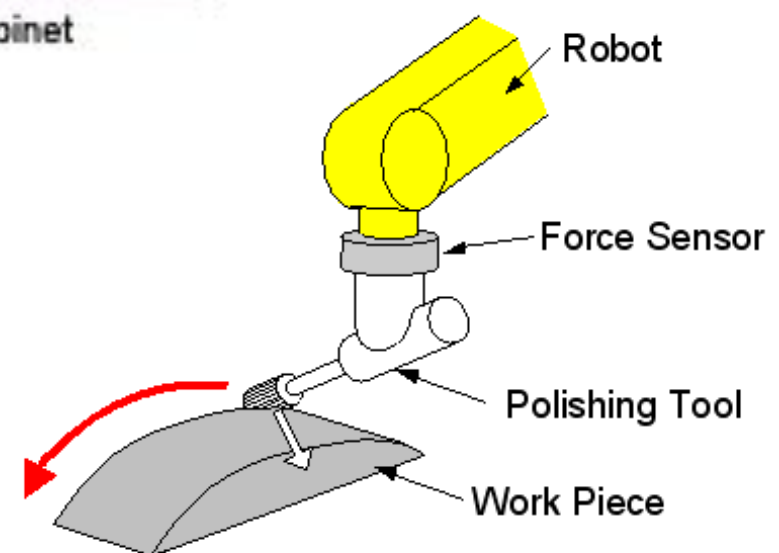
Phase matching by force sensing



Metal Cabinet



Gear Parts



Following with constant pushing force



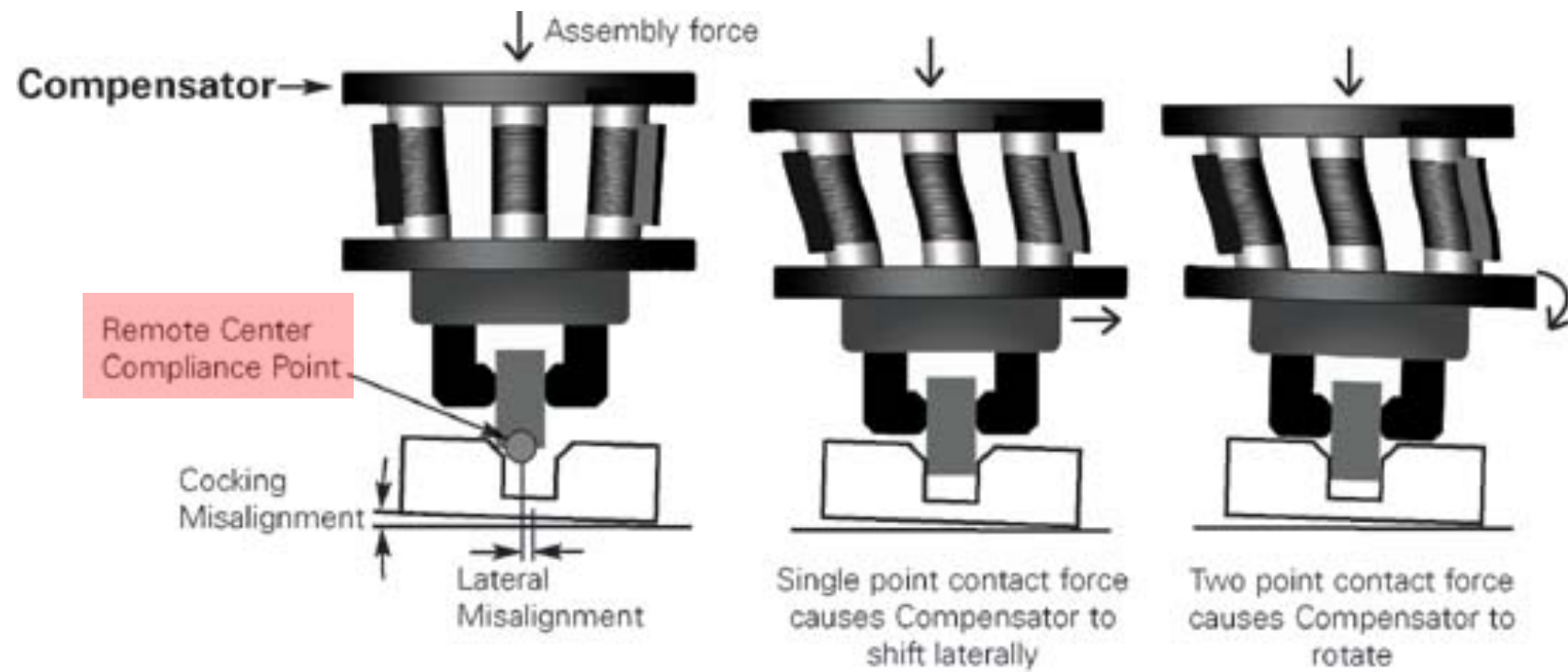
# Passive RCC device

- RCC = Remote Center of Compliance
- placed on the wrist so as to introduce **passive “compliance”** to the robot end-effector, in response to static forces and moments applied from the environment at the contact area
- mechanical construction yields “**decoupled**” linear/angular motion responses **if** contact occurs at or near the RCC point



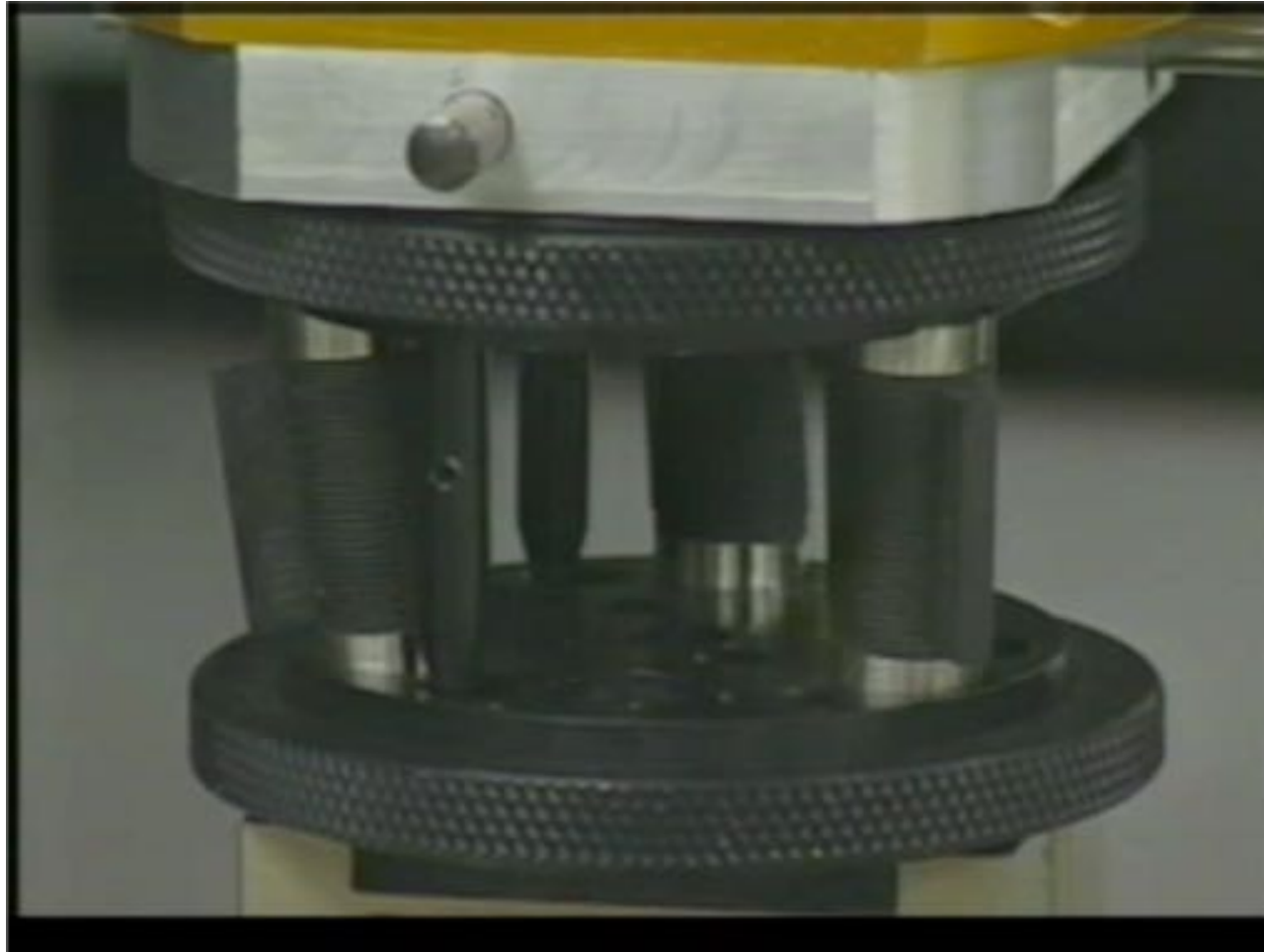


# Assembly with RCC





# Passive assembly with RCC



video

RCC by ATI Industrial Automation  
<http://www.ati-ia.com>



# Active assembly with F/T sensor

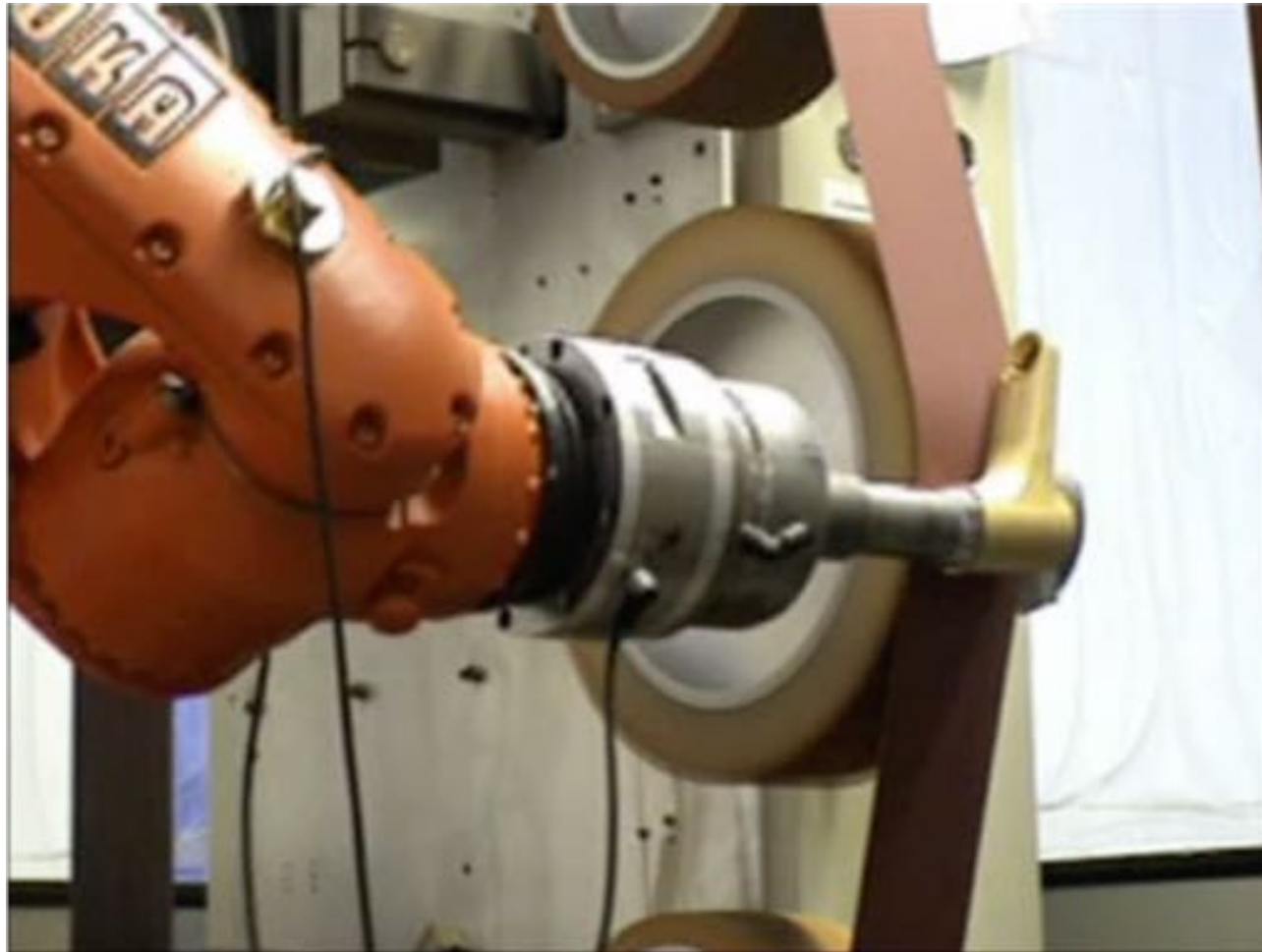


[video](#)

ABB robot with ATI F/T sensor



# Surface finishing with F/T sensor



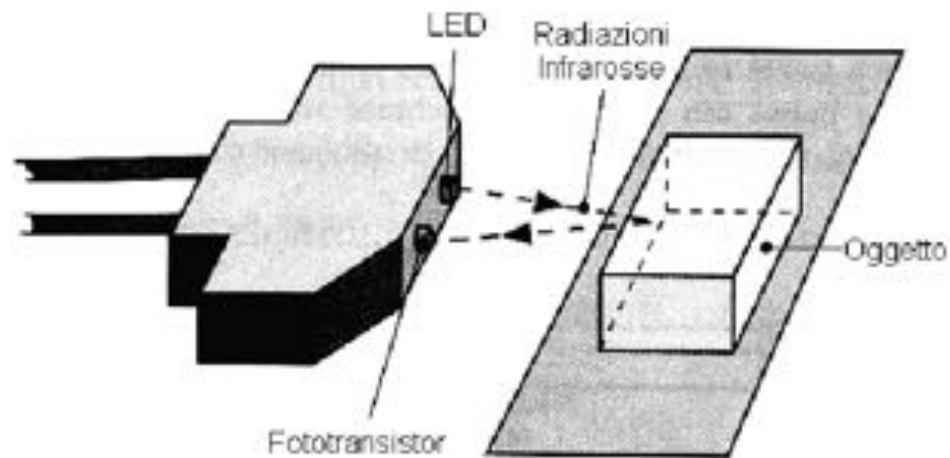
video

KUKA robot with F/T sensor



# Proximity/distance sensors - 1

- **infrared:** a light source (LED) emitting a ray beam (at  $850 \pm 70$  nm) which is then captured by a receiver (photo-transistor), after reflection by an object
- received intensity is related to distance
  - narrow emitting/receiving angle; use only indoor; reflectance varies with object color
- typical sensitive range:  $4 \div 30$  cm or  $20 \div 150$  cm
- cost: 15 €

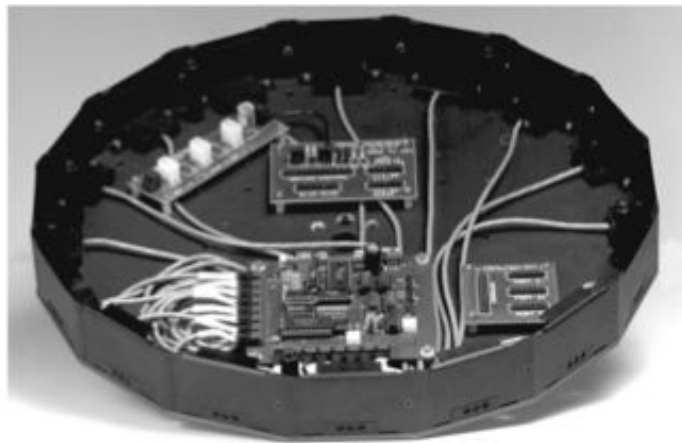


IR sensor SHARP GP2  
(supply 5V, range  $10 \div 80$  cm)



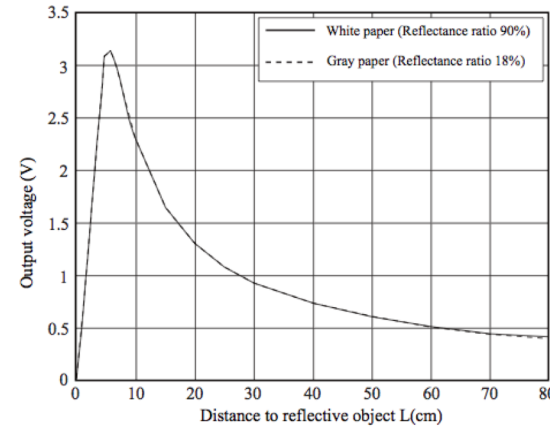
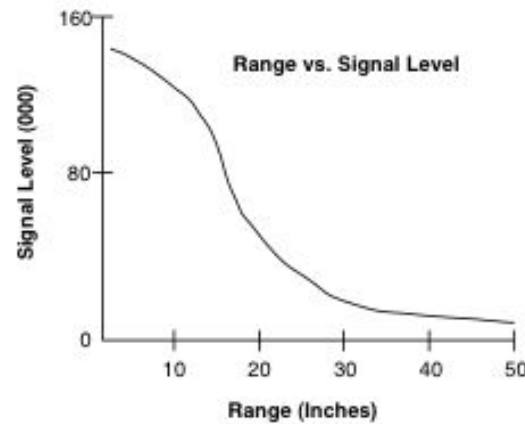
# Infrared sensor

example: Sensus 300  
on Nomad 200 mobile robot  
(power data: 500 mA at 12 V)

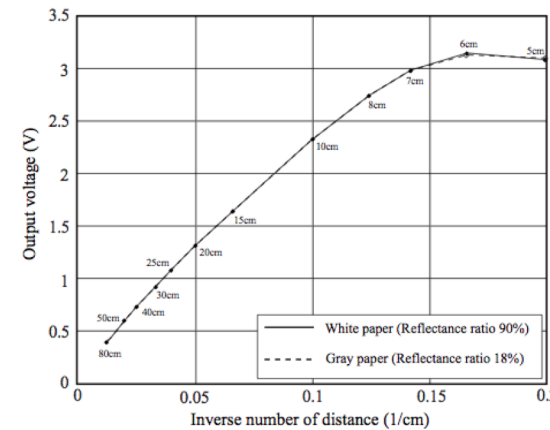


ring with 16 IR sensors

Sensus 300



Sharp GP2



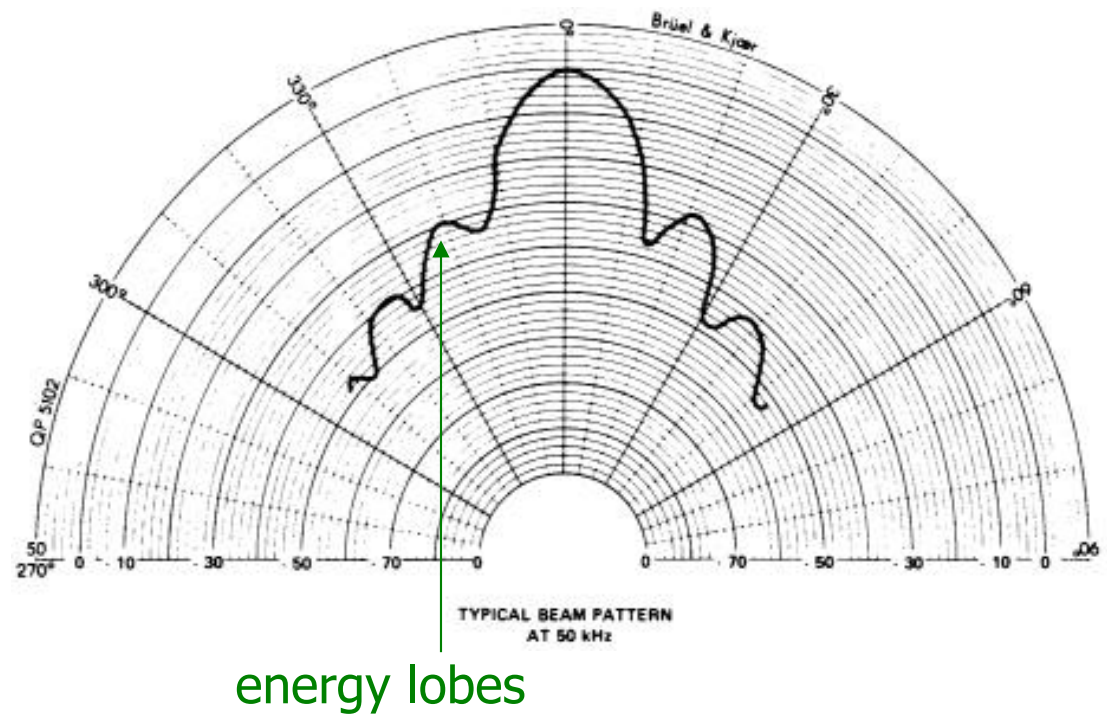
variation of received signal level as a direct or inverse function of distance



# Proximity/distance sensors - 2

- **ultrasound:** use of sound wave propagation and reflection (at  $> 20$  kHz, mostly 50 kHz), generated by a piezoelectric transducer excited by alternate voltage ( $V \sin \omega t$ )
- distance is proportional to the **Time-Of-Flight** (TOF) along the sensor-object-sensor path

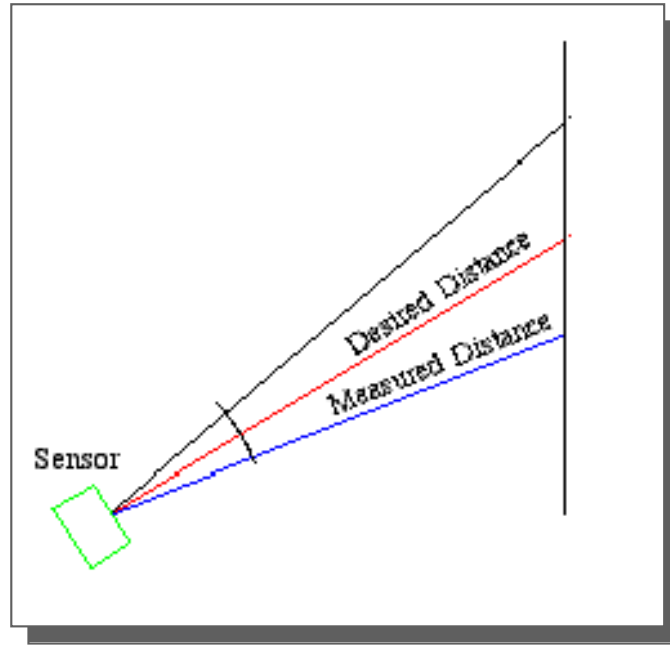
wave emitting angle  $\approx 30^\circ$   
allows to detect also obstacles located slightly aside from the front direction (but with uncertainty on their angular position)



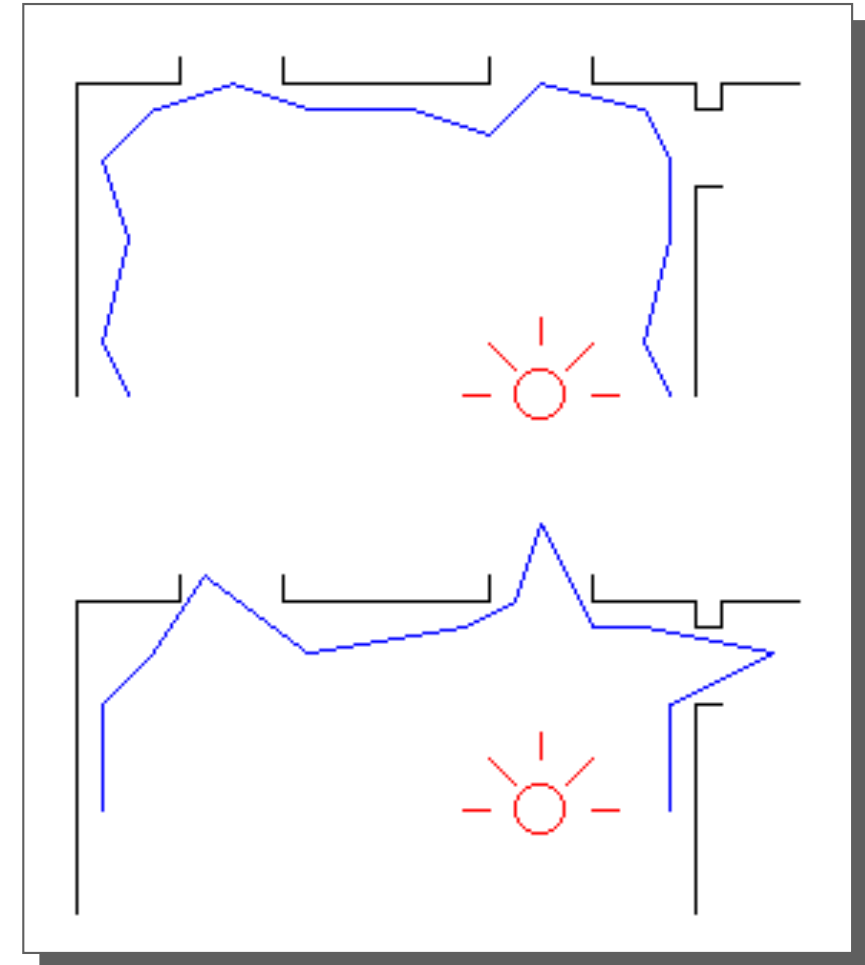


# Ultrasound sensor

some problems related to US wave propagation

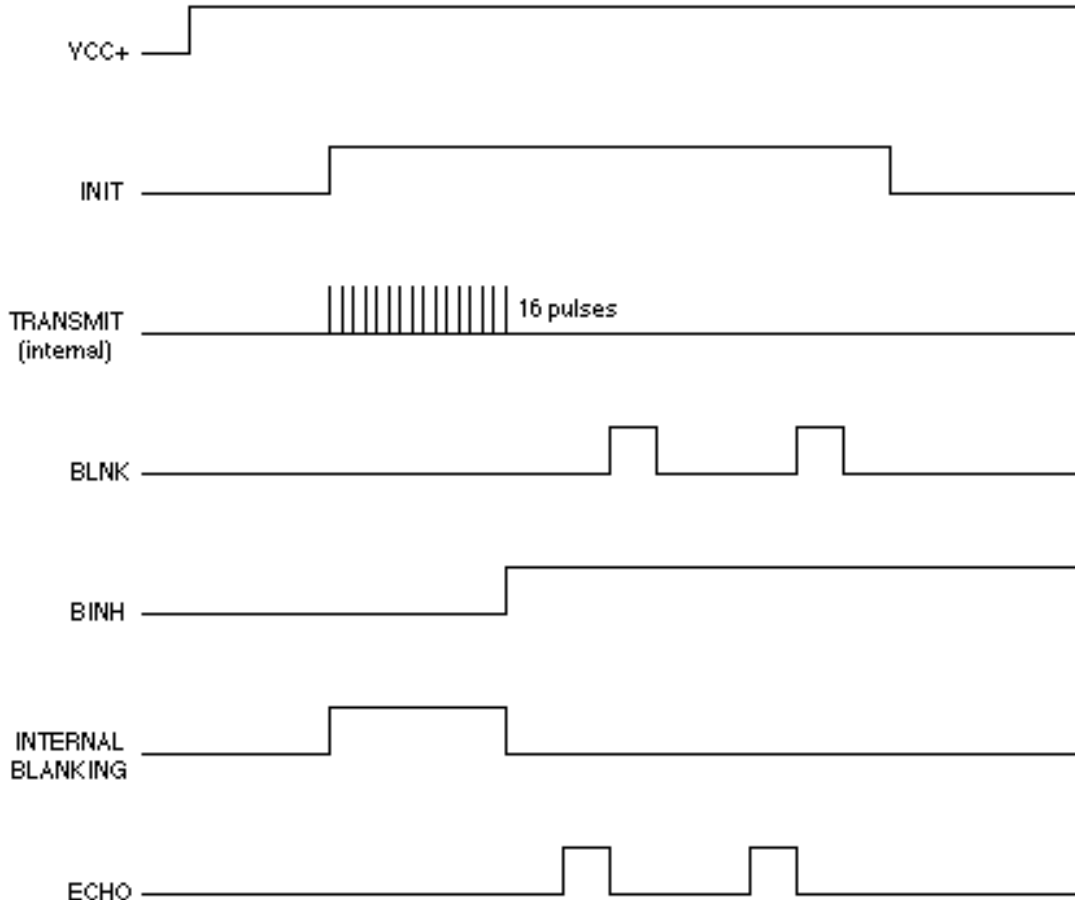


- uncertainty in distance evaluation within the cone of emission
- multiple reflections/echoes
- absorbing surfaces
- mirroring surfaces





# Range limits for US sensors



- during US pulses transmission the receiver is disabled, so as to avoid interferences that may lead to false readings
- the same is done after receiving the first echo, so as to avoid multiple reflections from the same object
- this limits the minimum distance that can be detected ( $> 0.5$  m)
- due to angular dispersion during emission, wave energy decreases with  $d^2$
- to compensate for this effect, the gain of the receiver is increased over time (up to a limit)
- max detectable distance  $\approx 6.5$  m



# Polaroid ultrasound sensor

- complete “kit” with trans-receiver and circuitry
- 3.5 ms of TOF for a front obstacle placed at 60 cm of distance
- range: 0.5÷2.5 m
- cost: < 30 €
- typical circular mounting of 16-32 US sensors (with a suitable sequence of activation)



Polaroid USP3

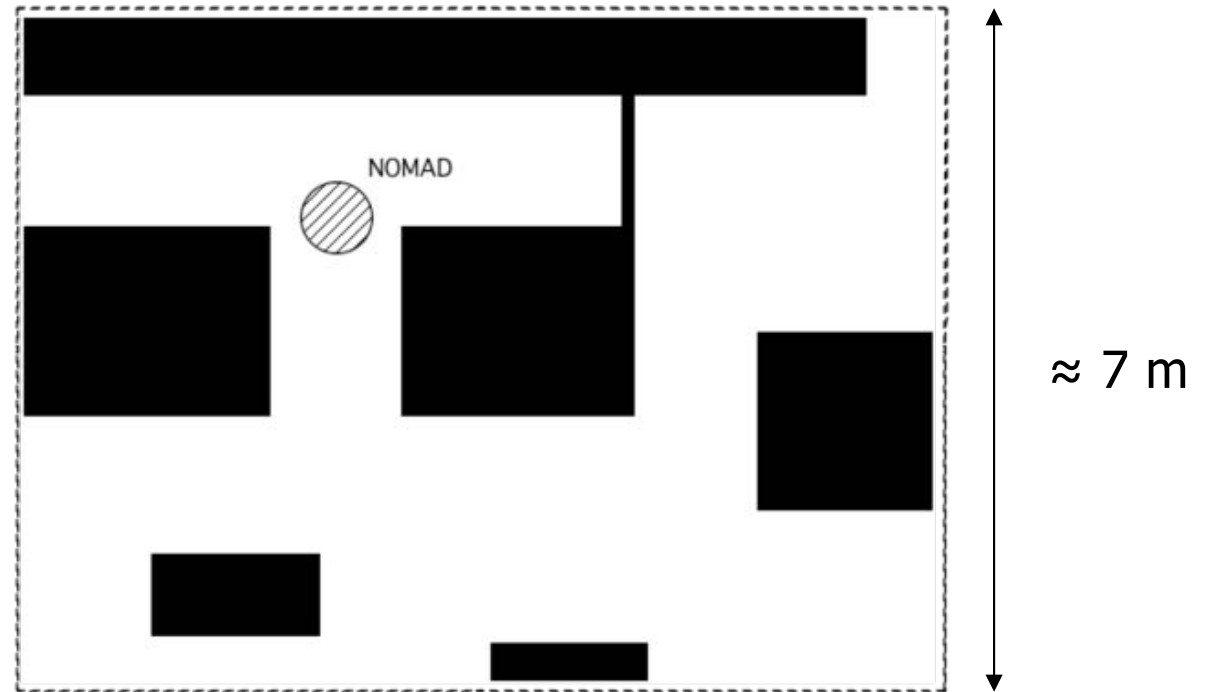


Migatron RPS 409



# Navigation with ultrasound sensing

- Nomad 200 with 16 US sensors (plus other not used here)

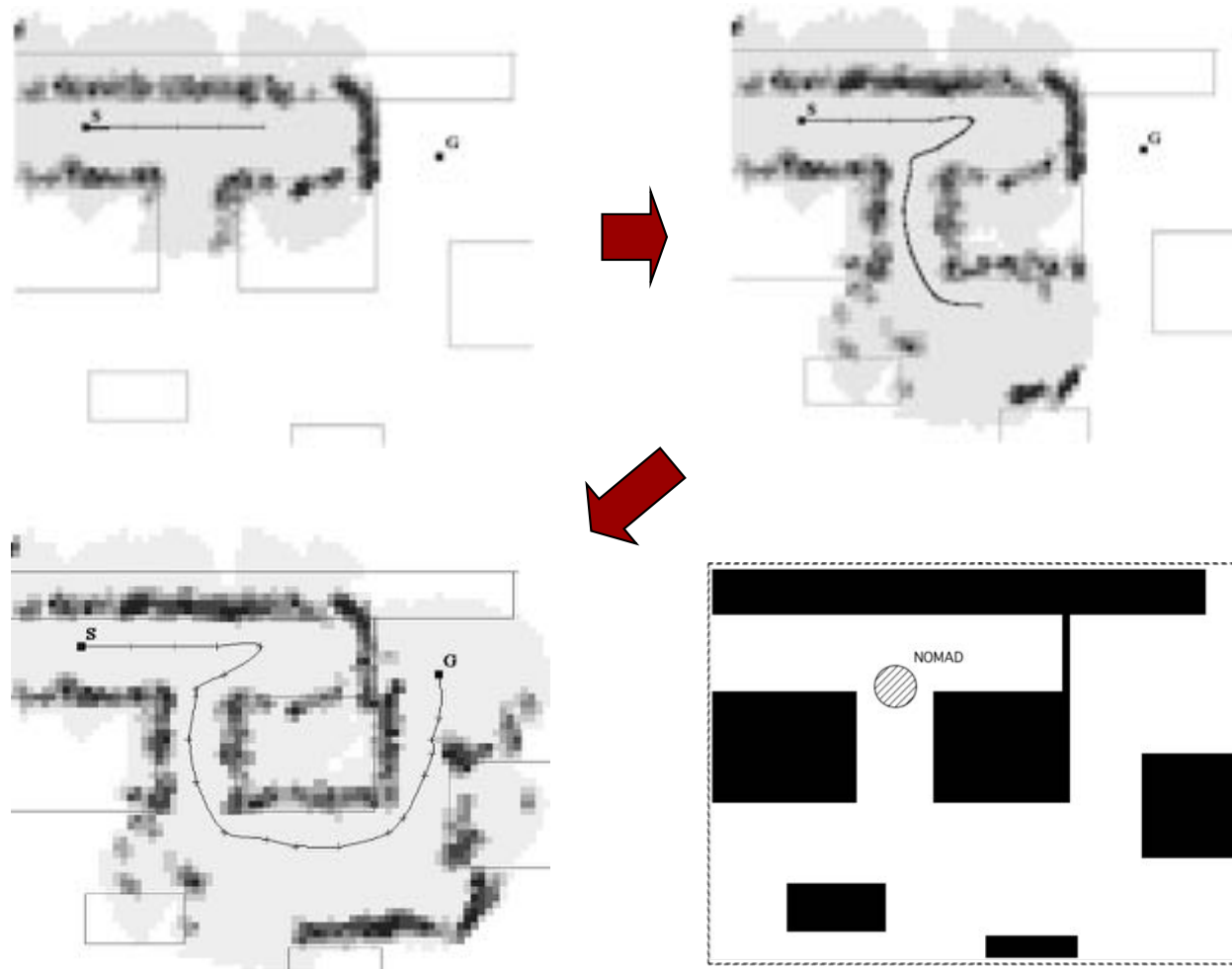


view of the robot and map of the former DIS Robotics Lab in Via Eudossiana 18  
(the map is initially unknown to the robot)



# Navigation with ultrasound sensing

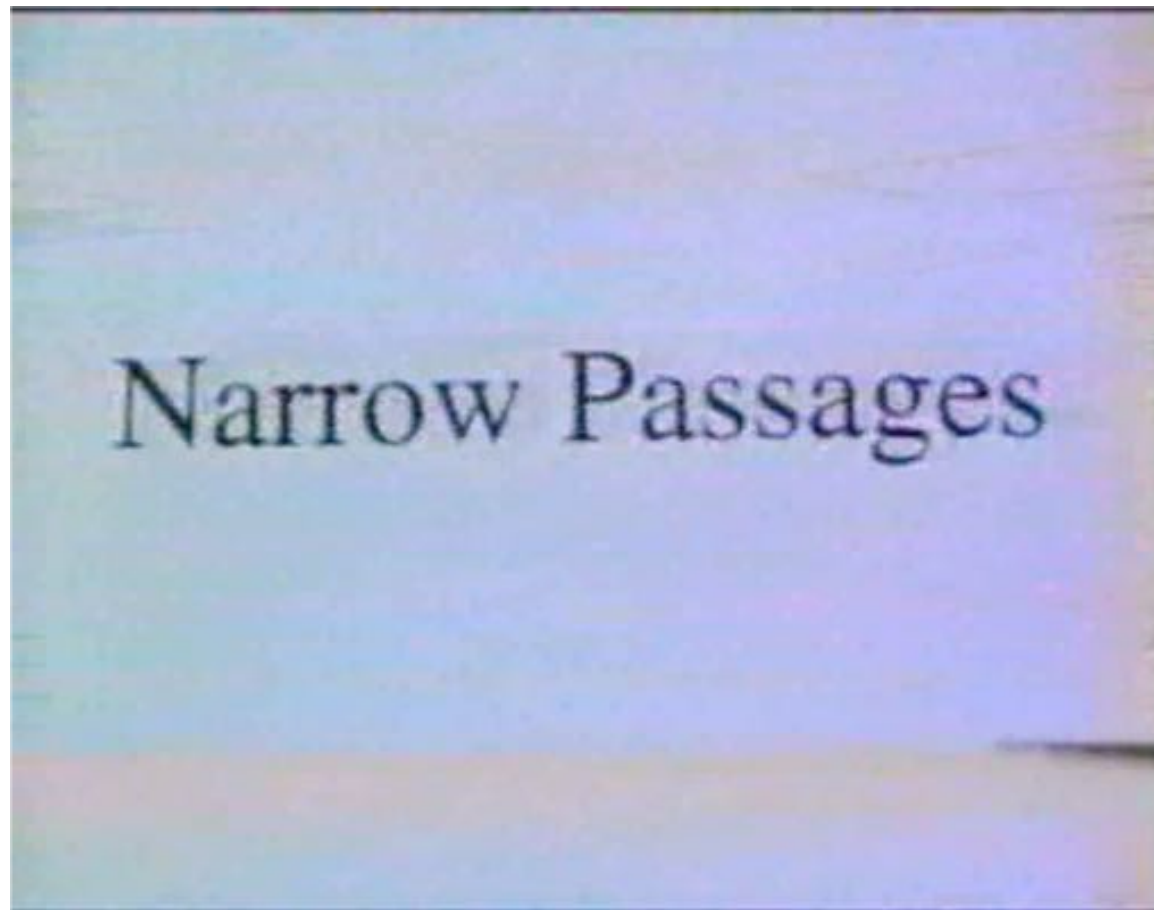
- grid map (unit = 10 cm) obtained by weighting successive data readings from US sensors with **fuzzy logic**; “aggressive” motion planning with **A\*** search algorithm on graphs; **reactive** US-based navigation to avoid unexpected obstacles





# Narrow passages

- Nomad 200 navigating with 16 ultrasonic sensors (old Robotics Lab, 1995)



video

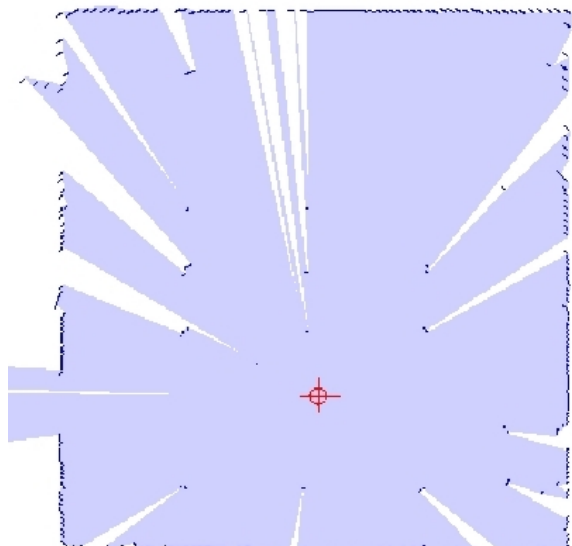


# Proximity/distance sensors – 3

- **laser scanner:** two-dimensional scan of the environment with a radial field of **infrared** laser beams (laser radar)
  - time between transmission and reception is directly proportional to the distance to the object (**Time-of-Flight**)

- **Sick LMS 200**

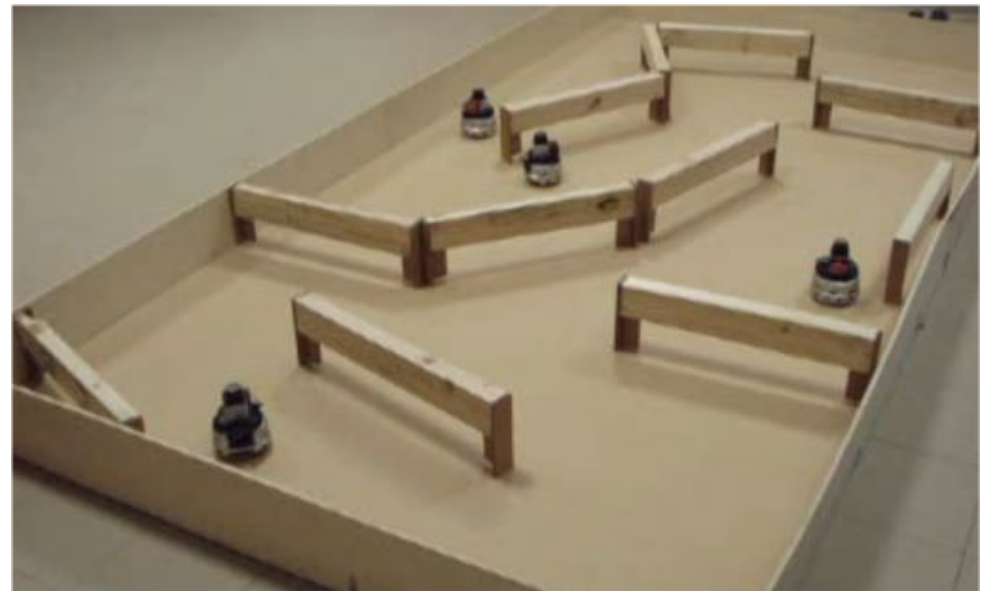
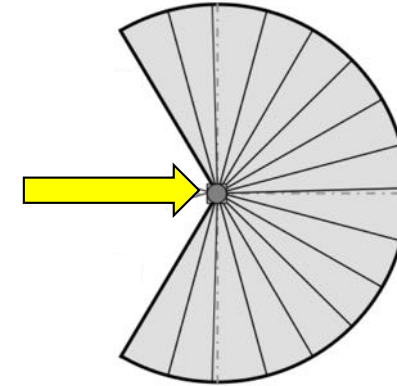
- wide angular range: max 180°
- high angular resolution that can be set by the user: 0.25° - 0.5° - 1°
- response time: 53 - 26 - 13 msec (depending on resolution)
- large range: 10 m up to 50÷80 m
- depth resolution:  $\pm 15$  mm
- interface: RS-232, RS-422
- used to be quite expensive (about 5000 €, this model now discontinued)





# A smaller laser scanner

- **Hokuyo URG-04X**
  - size:  $50 \times 50 \times 70$  mm
  - weight: 160 g
  - angular range: max 240°
  - angular resolution: 0.36°
  - response: 100 msec/scan
  - range: 0.02 ÷ 4 m
  - depth resolution:
    - ±1 cm (up to 1 m)
    - ±1% (beyond 1 m)
  - interface: RS-232, USB 2.0
  - supply: 5V DC
  - cost: 945 € (1080 US\$)
    - 2 years ago was 1750 € ...



4 small Khepera with Hokuyo sensors  
@ DIAG Robotics Lab



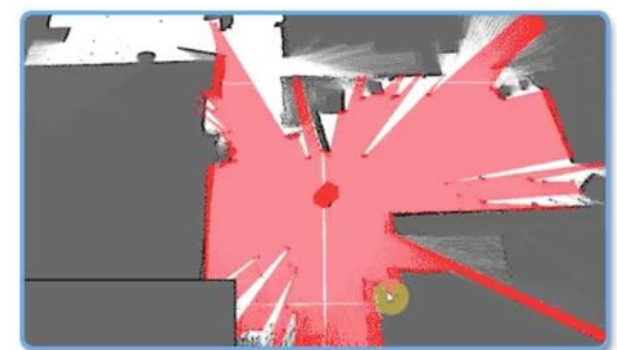
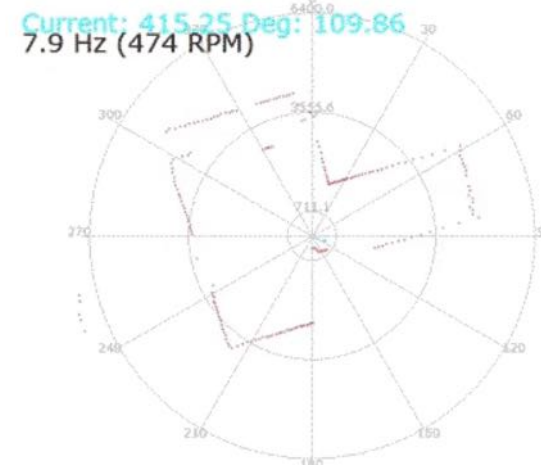
# Rotating laser scanner

## ■ RoboPeak RPLidar A1M1

- 360° 2D-scan, 6 m measurement range
- size: 70 × 98.5 × 60 mm
- weight: 200 g
- variable scanning rate: 2 ÷ 10 Hz
  - by varying the motor PWM signal
- angular resolution:  $\approx 1^\circ$  @5.5 Hz rate
  - 2000 samples/s @5.5 Hz rate
- depth resolution:  $\pm 20$  mm (0.2% of current depth)
- cost: 335 € (383 US\$) in development kit
- ROS & SLAM ready



RPLIDAR

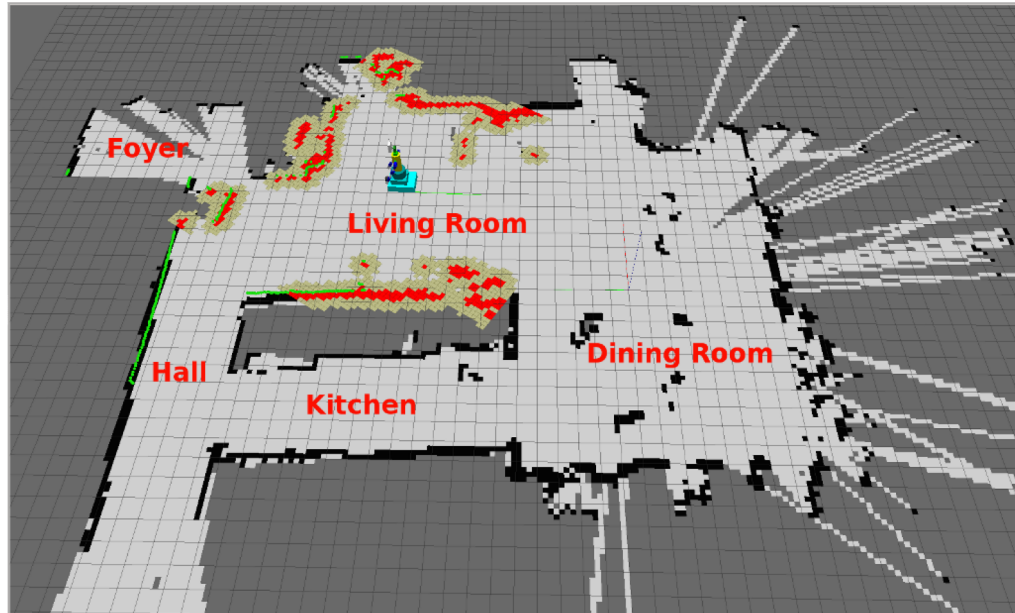


Realtime ICP-SLAM based on RPLIDAR



# Localization and mapping

- SLAM (Simultaneous Localization and Mapping) with a laser scanning sensor mounted on a mobile robot



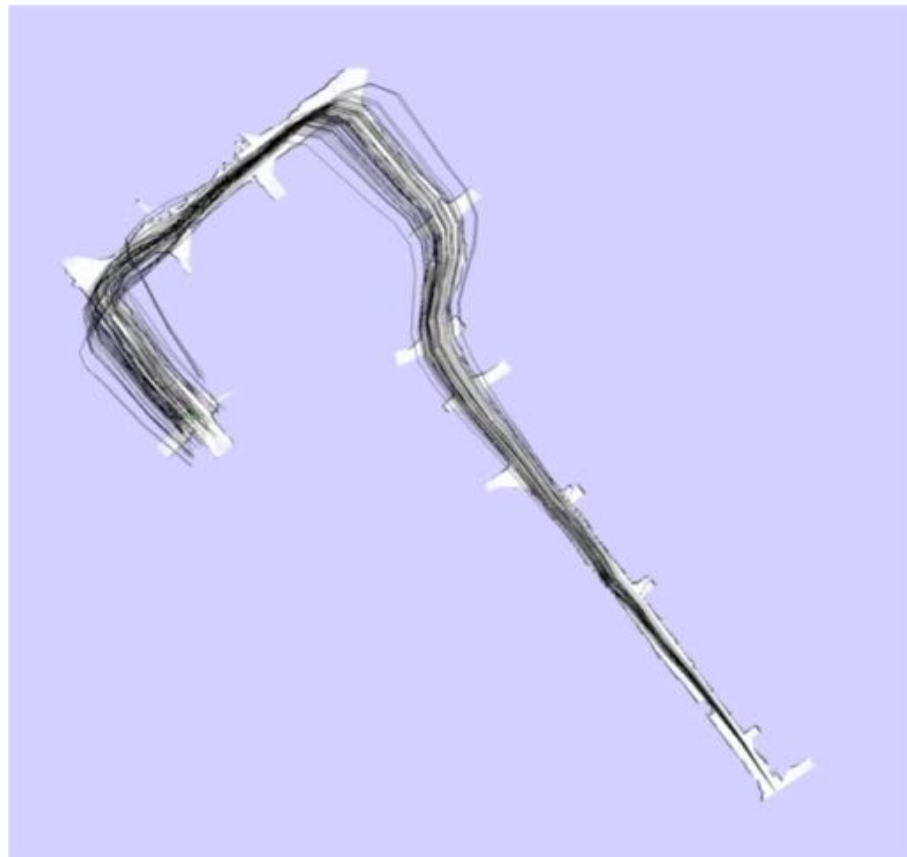
- An “extended” state estimation problem: determine at the same time
  - I. a map of the environment (sometimes, of its “landmarks” only)
  - II. the robot location within the mapusing an incremental, iterative measurement process (large scale data)



# Localization and mapping

illustrating the benefit of “loop closure” on long range data (map correction)

[video](#)



single loop

[video](#)

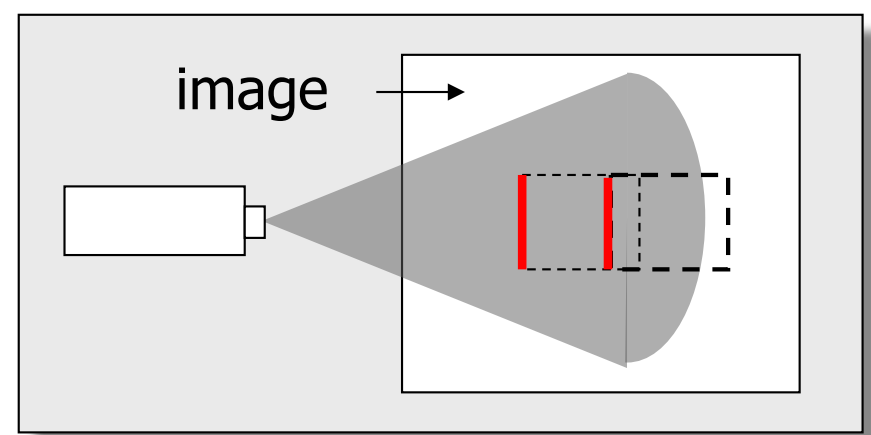
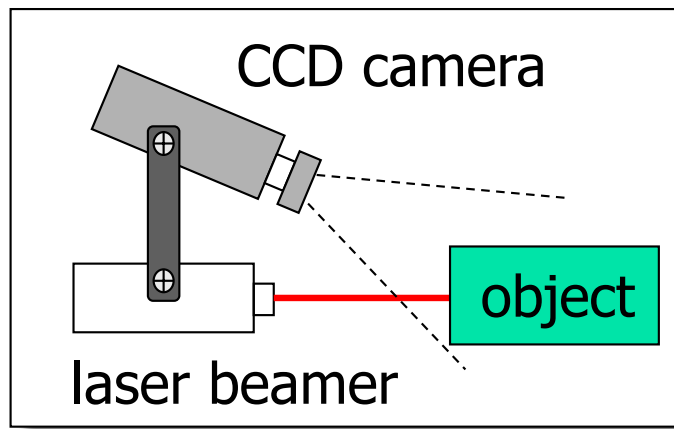


multiple loops (MIT Campus)

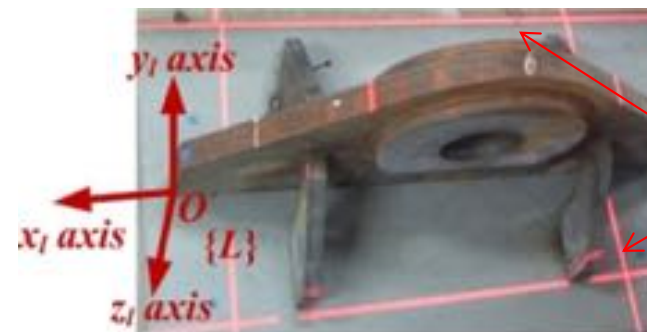


# Proximity/distance sensors - 4

- **structured light:** a laser beam (coherent light source) is projected on the environment, and its planar intersection with surrounding objects is detected by a (tilted) camera
- the position of the “red pixels” on the camera image plane is in **trigonometric** relation with the object distance from the sensor



side view



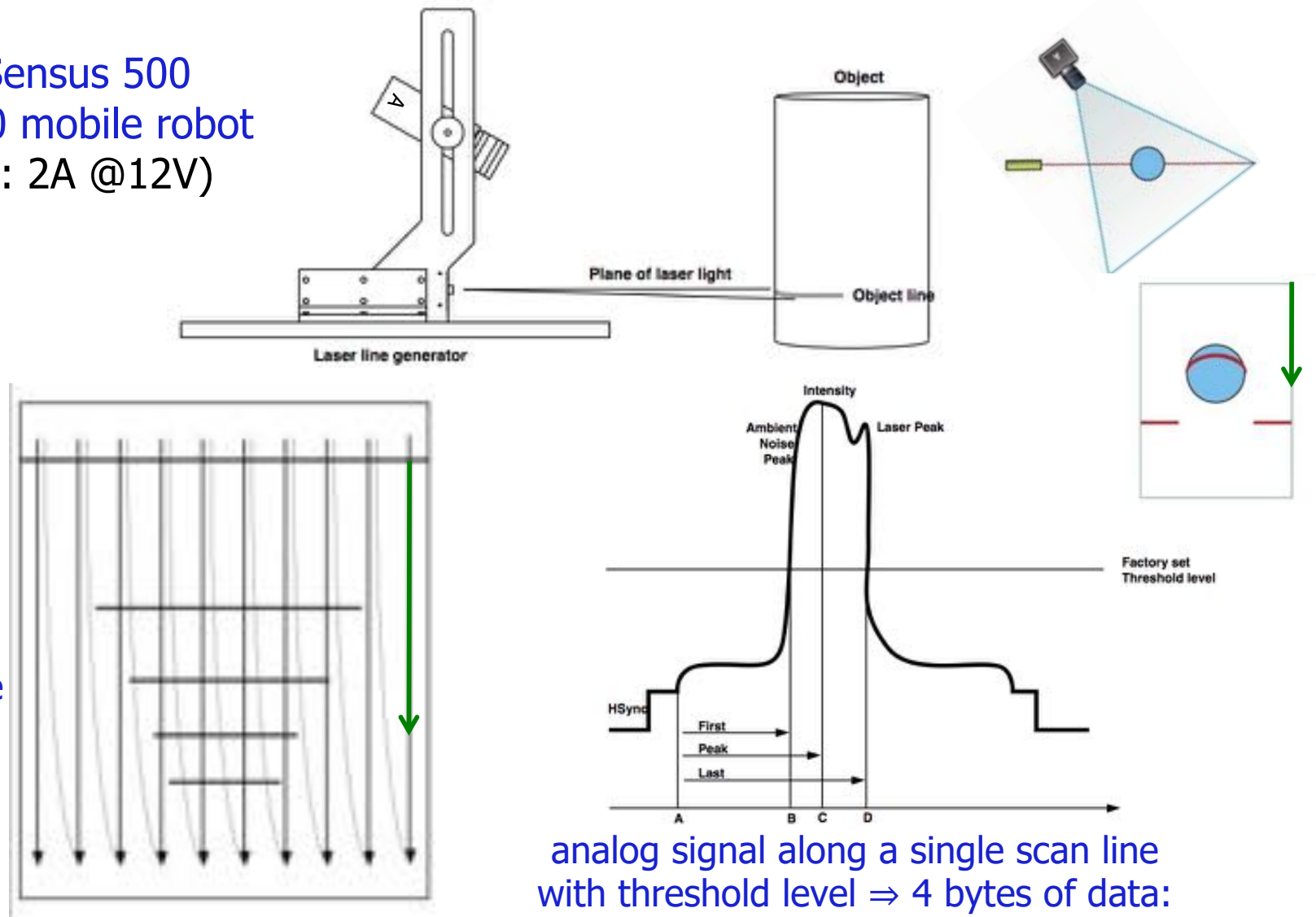
projected laser beams  
(2D in this case)

top view



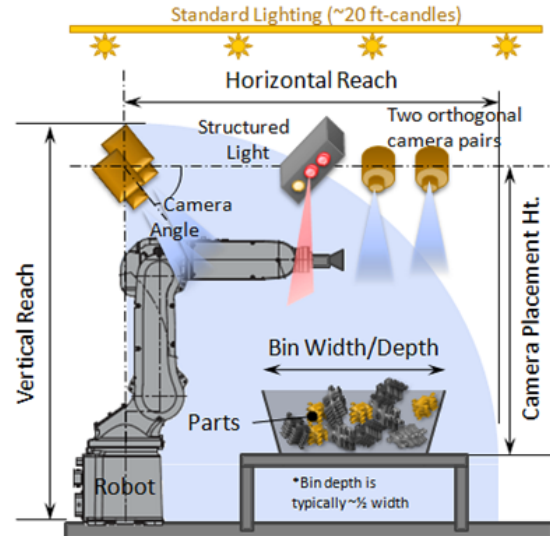
# Structured light sensor

example: Sensus 500  
on Nomad 200 mobile robot  
(power data: 2A @12V)





# Use of structured light sensors



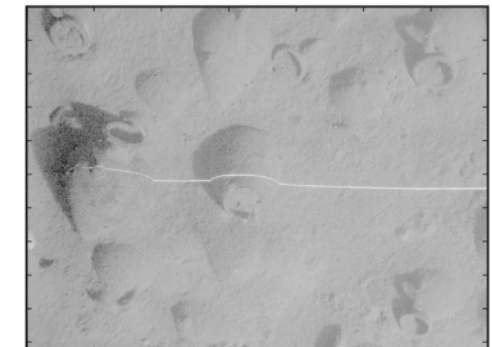
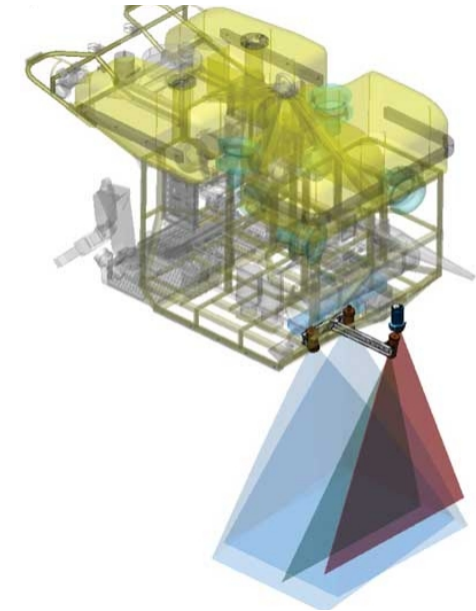
Random **bin picking** of 10-30 parts/minute (with surface inspection) with a 6R industrial robot, two pairs of cameras and a structured light sensor [Universal Robotics]



Structured light approach to best fit and **finish car bodies** (down to 0.1 mm) for reducing wind noise [Ford Motor Co.]



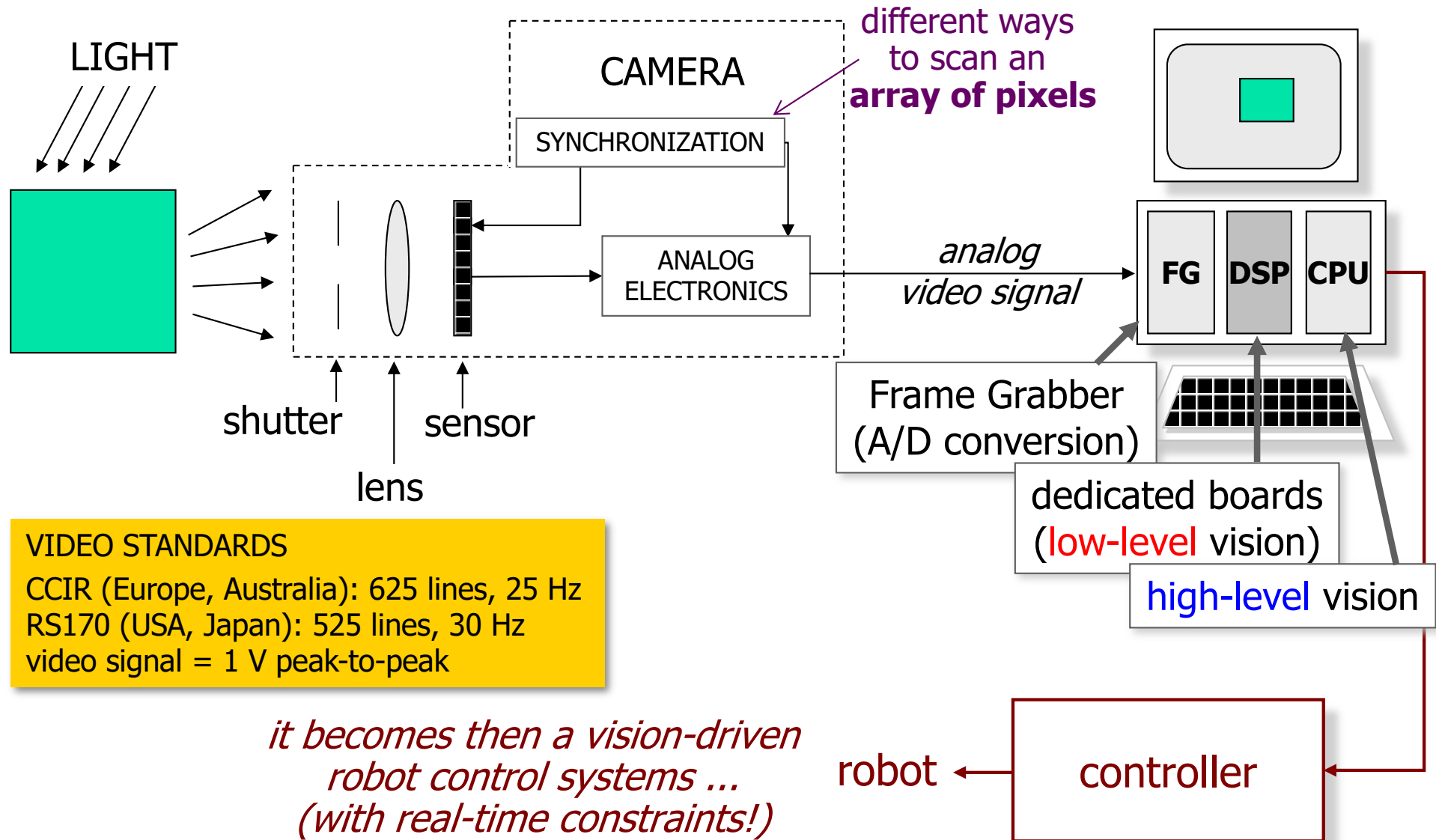
**Virtobot** system for post-mortem 3D optical scanning of human body & image-guided needle placement [Univ. Zürich]



**Hercules ROV** + structured-laser-light imaging system for high-resolution bathymetric underwater maps [Univ. Rhode Island]



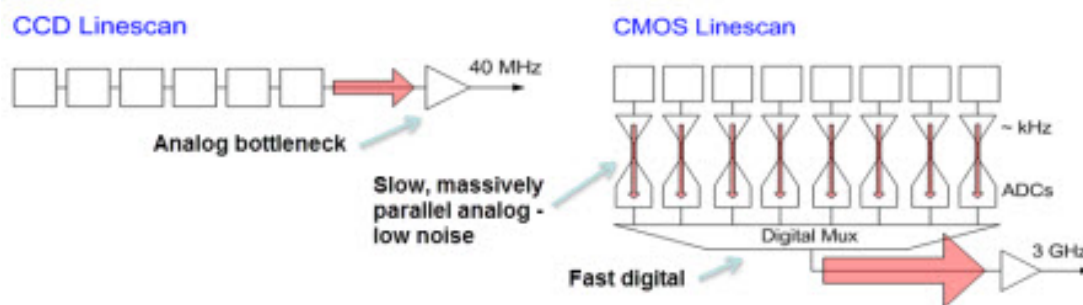
# Vision systems





# Sensors for vision

- arrays (spatial sampling) of photosensitive elements (**pixel**) converting light energy into electrical energy
- **CCD** (Charge Coupled Device): each pixel surface is made by a semiconductor device, **accumulating** free charge when hit by photons (**photoelectric effect**); “integrated” charges “read-out” by a sequential process (external circuitry) and transformed into voltage levels
- **CMOS** (Complementary Metal Oxide Semiconductor): each pixel is a **photodiode**, directly providing a voltage or current proportional to the **instantaneous** light intensity, with possibility of random access to each pixel





# CMOS versus CCD

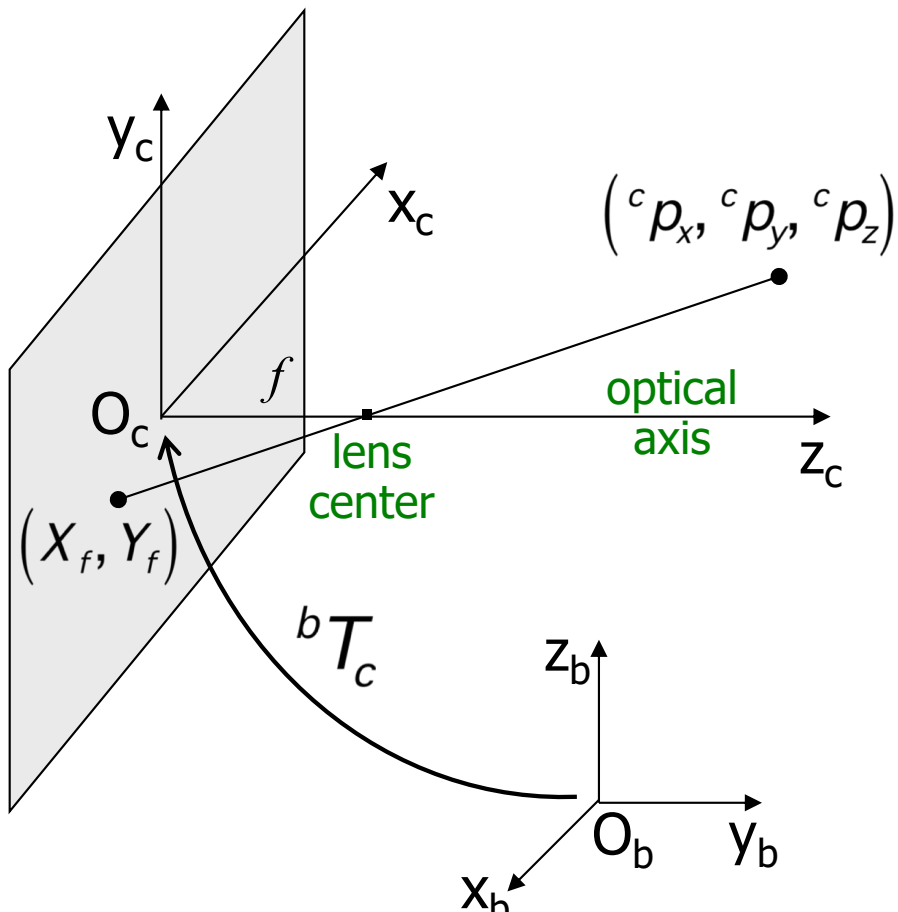
---

- reduction of fabrication costs of CMOS imagers
- better spatial resolution of elementary sensors
  - CMOS: 1M pixel, CCD:  $768 \times 576$  pixel
- faster processing speed
  - 1000 vs. 25 fps (frames per second)
- possibility of integrating “intelligent” functions on single chip
  - sensor + frame grabber + low-level vision
- random access to each pixel or area
  - flexible handling of ROI (Region Of Interest)
- possibly lower image quality w.r.t. CCD imagers
  - sensitivity, especially for applications with low S/N signals
- customization for small volumes is more expensive
  - CCD cameras have been since much longer time on the market



# Perspective transformation

image plane (with **camera frame**)



1. in metric units

$$X_f = \frac{f^c p_x}{f - {}^c p_z} \quad Y_f = \frac{f^c p_y}{f - {}^c p_z}$$

Robotics 1

2. in pixel

$$X_I = \frac{\alpha_x f^c p_x}{f - {}^c p_z} + X_0$$

offsets of pixel coordinate system w.r.t. optical axis

$$Y_I = \frac{\alpha_y f^c p_y}{f - {}^c p_z} + Y_0$$

pixel/metric scaling factor

3. LINEAR MAP in homogeneous coordinates

$$X_I = \frac{X_I}{Z_I} \quad Y_I = \frac{Y_I}{Z_I} \quad \rightarrow \quad \begin{bmatrix} X_I \\ Y_I \\ Z_I \end{bmatrix} = \Omega \begin{bmatrix} {}^c p_x \\ {}^c p_y \\ {}^c p_z \\ 1 \end{bmatrix}$$

$$\Omega = \begin{bmatrix} \alpha_x & 0 & X_0 & 0 \\ 0 & \alpha_y & Y_0 & 0 \\ 0 & 0 & 1 & 0 \end{bmatrix} \begin{bmatrix} 1 & 0 & 0 & 0 \\ 0 & 1 & 0 & 0 \\ 0 & 0 & -1/f & 1 \\ 0 & 0 & 0 & 1 \end{bmatrix}$$

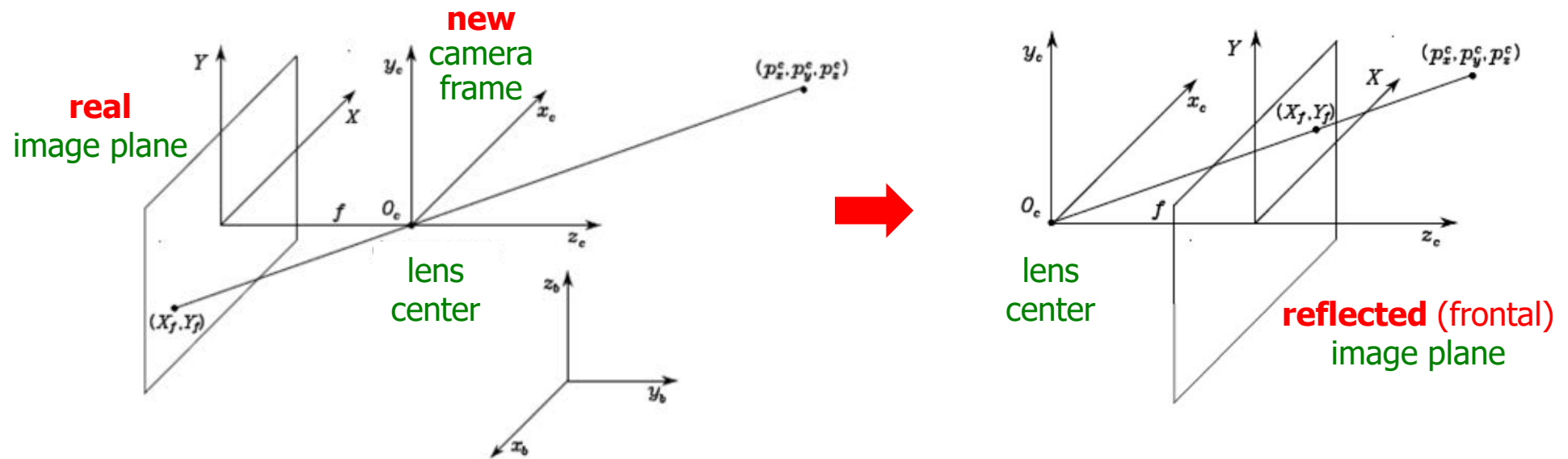
calibration matrix

$$H = \Omega \ {}^c T_b$$

intrinsic and extrinsic parameters



# Perspective transformation with camera frame at the lens center



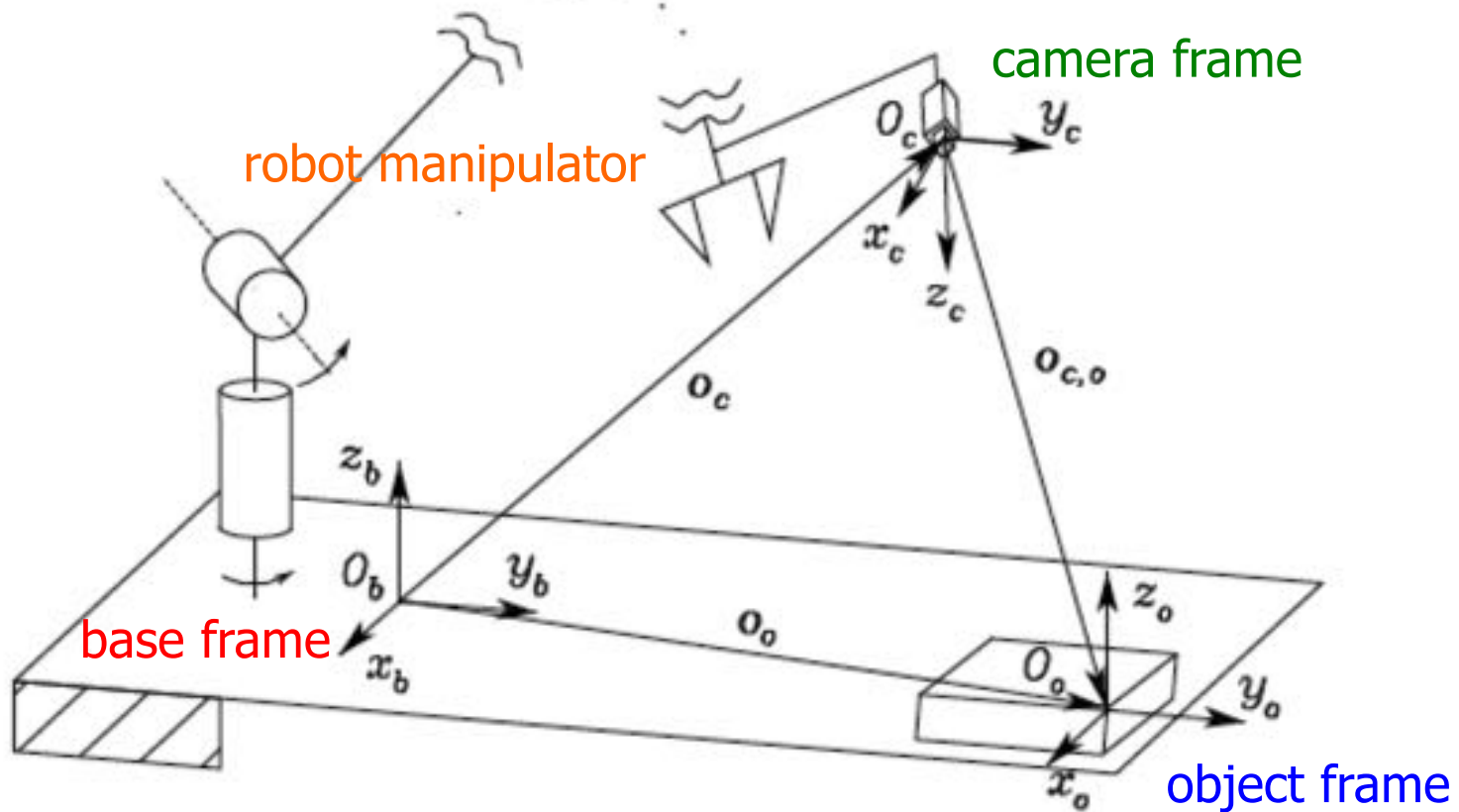
1. in metric units  $X_f = -\frac{f^c p_x}{c p_z} \quad Y_f = -\frac{f^c p_y}{c p_z}$   $\rightarrow$   $X_f = \frac{f^c p_x}{c p_z} \quad Y_f = \frac{f^c p_y}{c p_z}$

2. in pixel  $\dots$   $\rightarrow$   $X_I = \frac{\alpha_x f^c p_x}{c p_z} + X_0 \quad Y_I = \frac{\alpha_y f^c p_y}{c p_z} + Y_0$

3. LINEAR MAP in homogeneous coordinates  $\dots$   $\rightarrow$   $\begin{bmatrix} x_I \\ y_I \\ z_I \\ 1 \end{bmatrix} = \Omega \begin{bmatrix} c p_x \\ c p_y \\ c p_z \\ 1 \end{bmatrix} \quad \Omega = \begin{bmatrix} \alpha_x f & 0 & X_0 & 0 \\ 0 & \alpha_y f & Y_0 & 0 \\ 0 & 0 & 1 & 0 \end{bmatrix}$



# Eye-in-hand camera



Relevant reference frames for visual-based tasks

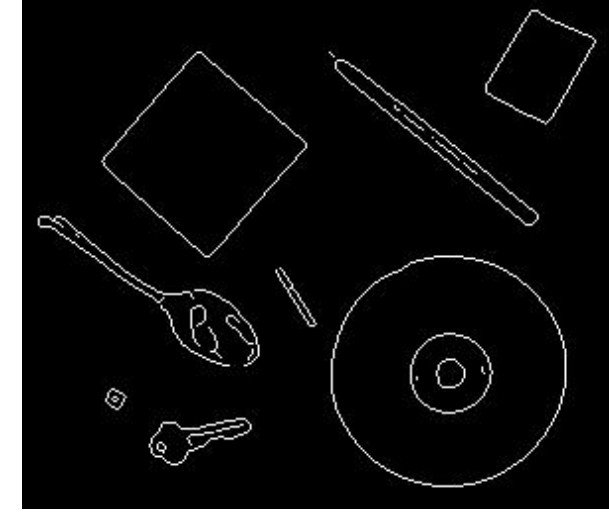


# Low-level vision

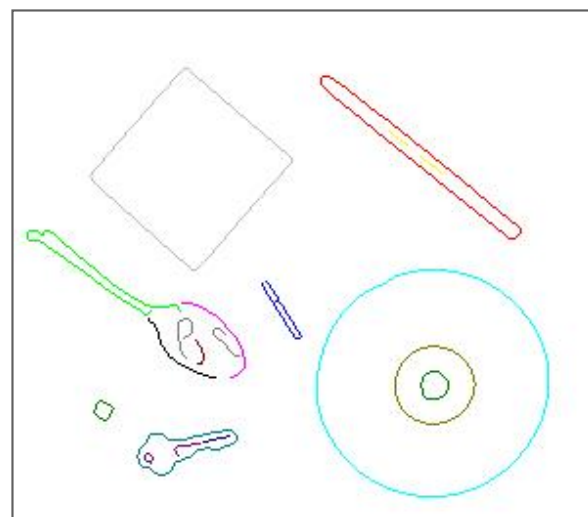
## contour reconstruction



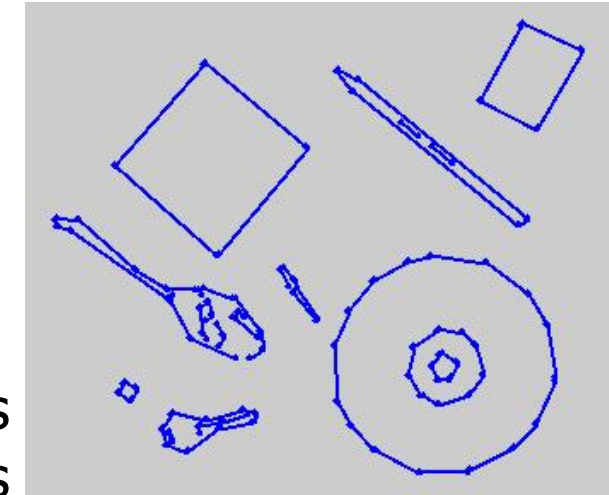
original image



edge detection



adjacent pixels on  
the edges are  
connected  
and labeled with  
different colors



linear segments  
fitted to the edges



# High-level vision

## features matching in stereovision

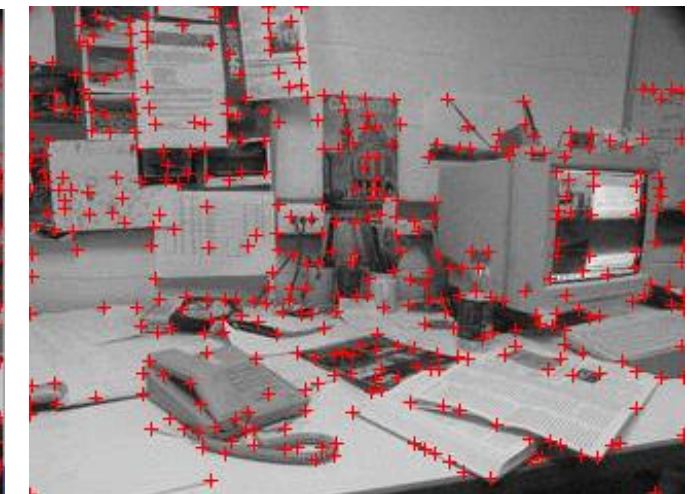
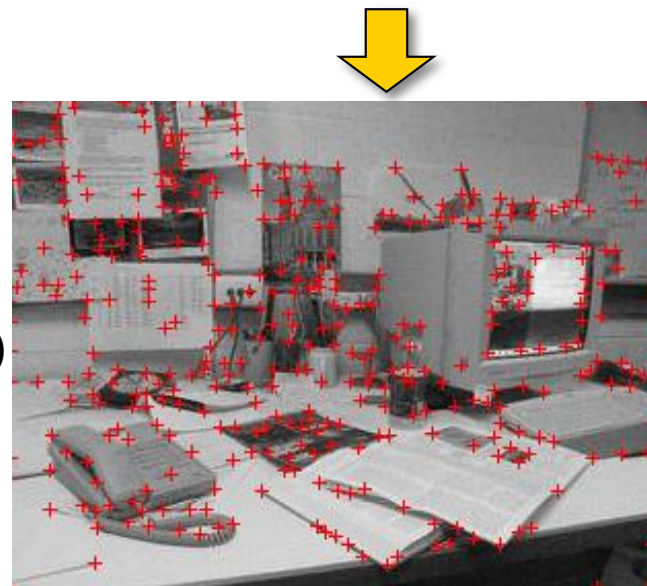


**goal:** find the  
“fundamental matrix”  
(rigid transformation  
between the two images)  
**use:** visual localization



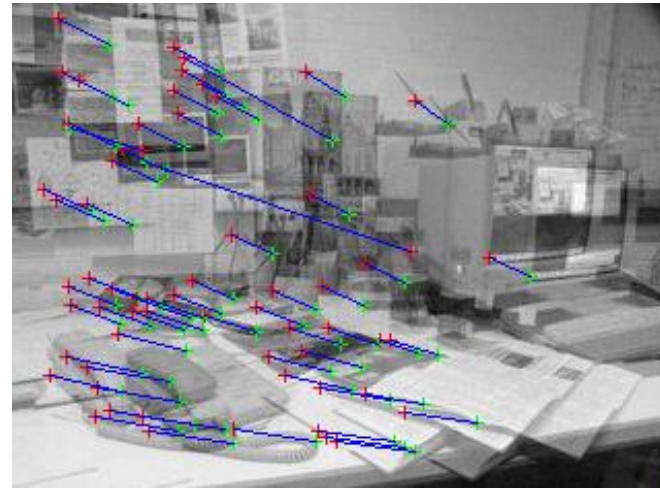
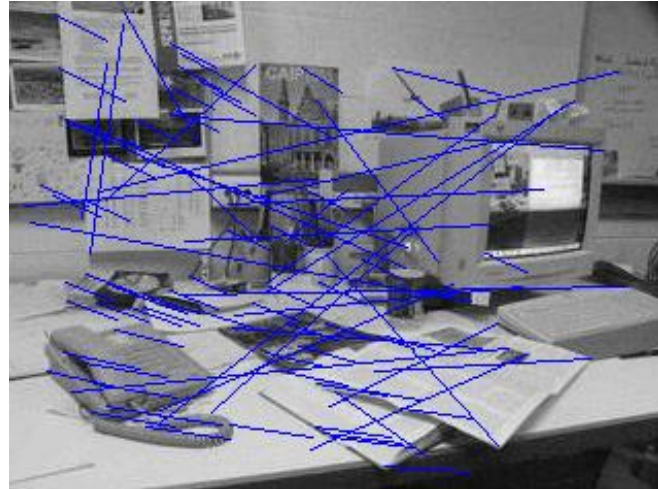
L- and R-views acquired, e.g.,  
by stereocamera **Videre** ( $\approx 5\text{cm}$ )

corners in the two images  
(in general, “features”)



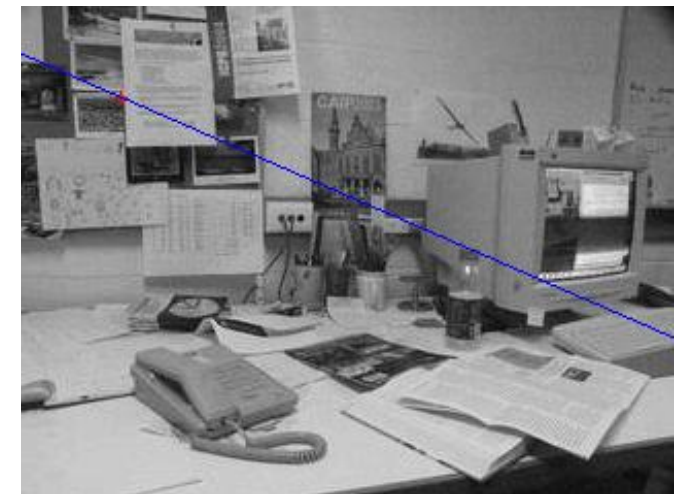
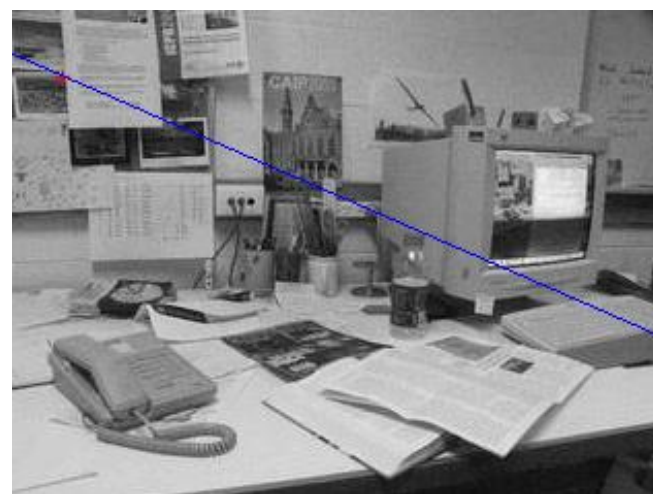


# High-level vision (cont)



**left:** correspondence hypotheses used to find the best fitting fundamental matrix  
**right:** inconsistent correspondences are eliminated

corresponding line  
in the two images



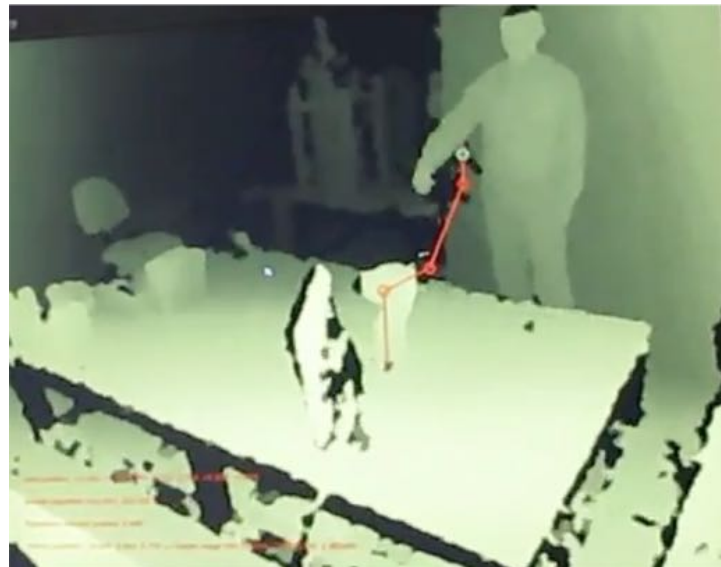


# Kinect

## camera + structured light 3D sensor



Kinect 2.0



- RGB camera (with  $640 \times 480$  pixel)
- depth sensor (by PrimeSense)
- infrared laser emitter
- infrared camera (with  $320 \times 240$  pixel)
- 30 fps data rate
- range:  $0.5 \div 5$  m
- depth resolution: 1cm@2m; 7cm@5m
- cost: < 90 €

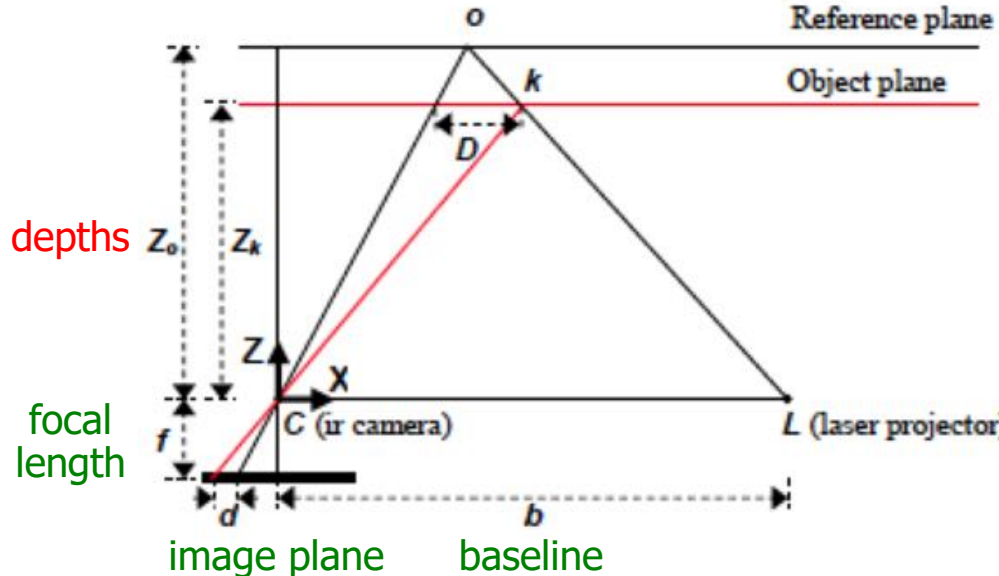


“skeleton” extraction and  
human motion tracking



# Kinect

## Depth sensor operation



- stereo triangulation based on IR source emitting *pseudo-random* patterns
- reference pattern on IR camera image plane acquired in advance from a plane at known **distance** and coded in H/W
- correlating the disparity  **$d$**  (10 bits) of reference and received object patterns provides the **object depth  $Z_k$**

1. **triangulation** equations (by similarity of triangles)

$$\frac{D}{b} = \frac{Z_0 - Z_k}{Z_0} + \frac{d}{f} = \frac{D}{Z_k} \rightarrow$$

$$Z_k = \frac{Z_0}{1 + \frac{d}{fb} Z_0} \quad \begin{matrix} \rightarrow \\ X_k = -\frac{Z_k}{f}(x_k - x_0 + \delta x) \end{matrix}$$

$$\quad \begin{matrix} \rightarrow \\ Y_k = -\frac{Z_k}{f}(y_k - y_0 + \delta y) \end{matrix}$$

2. accurate **calibration** of sensor

baseline length  $b$ , depth of reference  $Z_0$  + camera **intrinsic** parameters  
(focal length  $f$ , lens distortion coefficients  $\delta x, \delta y$ , center offsets  $x_0, y_0$ )



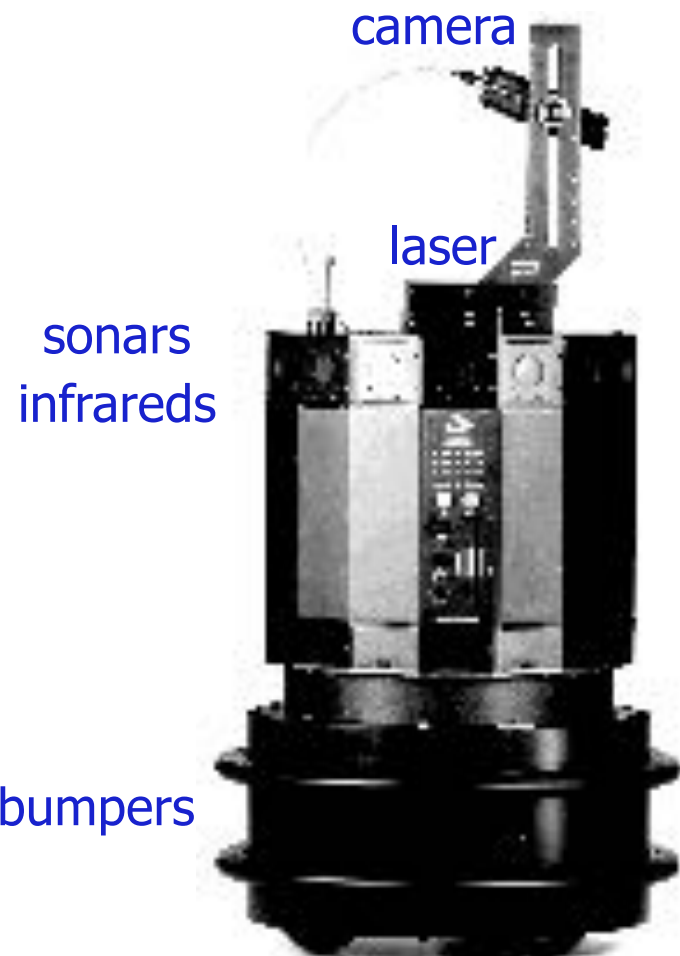
# How Kinect works (a 2-minute illustration...)



<http://youtu.be/uq9SEJxZiUg>



# Nomad 200 mobile robot



- structured light vision system (laser + CCD camera)
  - 480 scan lines/frame, 30 fps
  - range: 45÷300 cm
- 16 sonar sensors (Polaroid 50 KHz)
  - each with a field of view of 25°
  - range: 40÷640 cm, resolution 1%
- 16 infrared sensors
  - range: ≤ 60 cm, readings every 2.5 msec
- 20 pressure-sensitive bumpers
- radio-ethernet communication



# Magellan Pro mobile robot

---

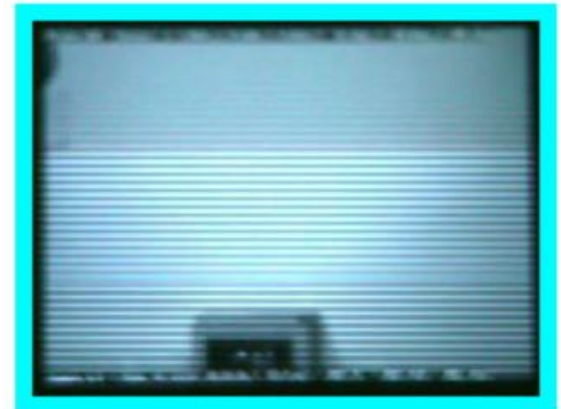
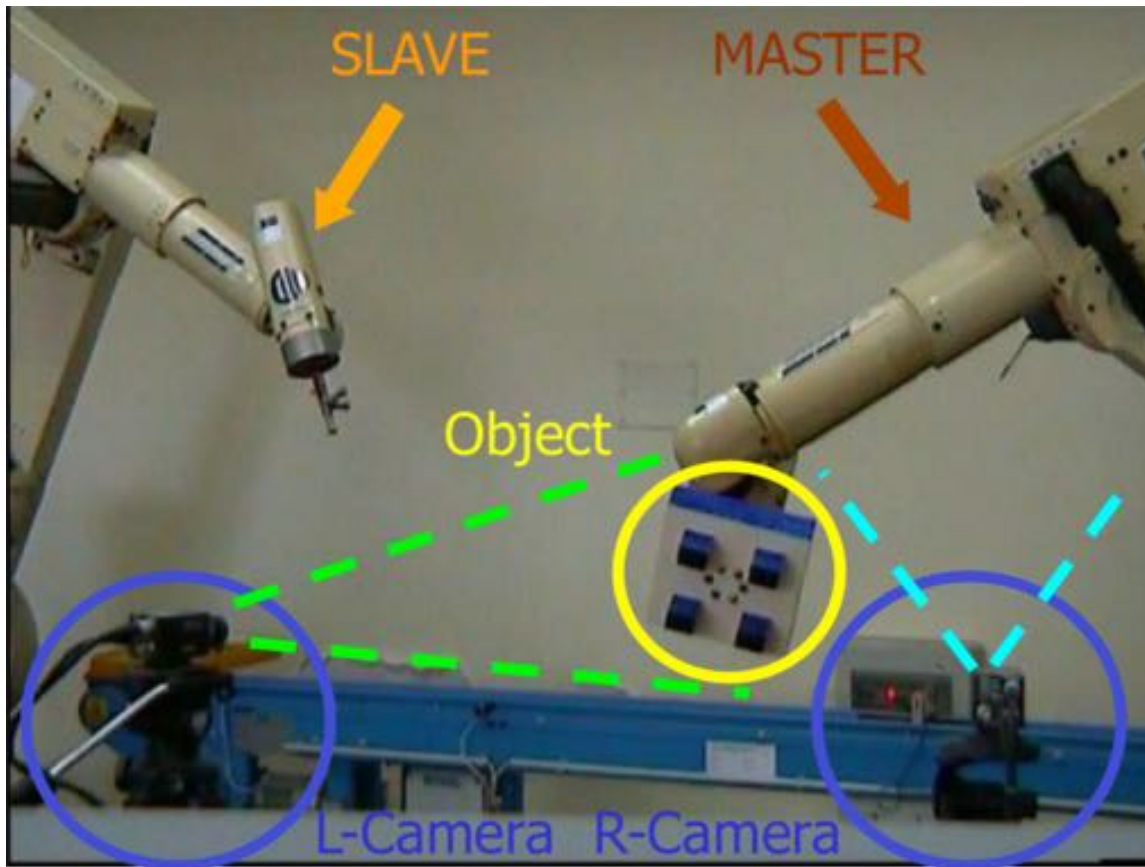


- pan-tilt color camera (7 Hz...)
- 16 sonar sensors
- 16 infrared sensors
- 16 pressure-sensitive bumpers
- ethernet radio-link



# Manipulators and vision systems

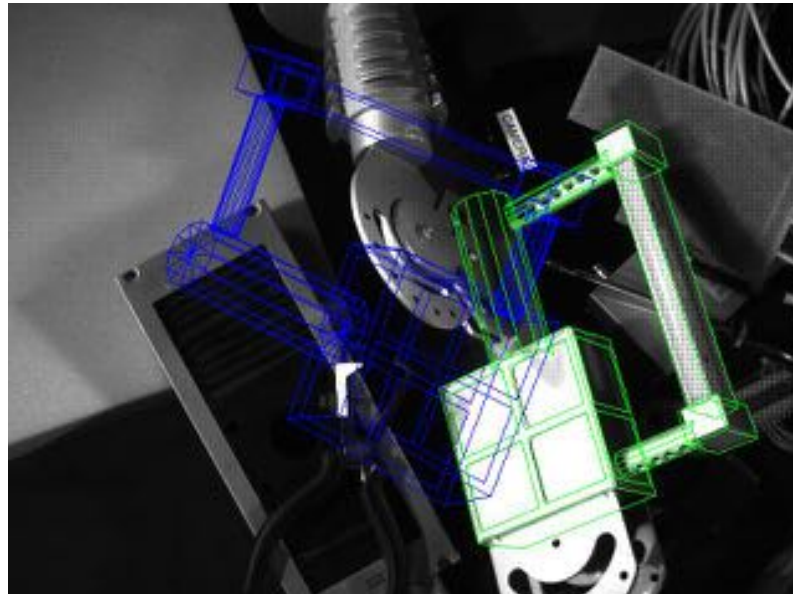
- stereovision with two external cameras, fixed in the environment (**eye-to-hand**)





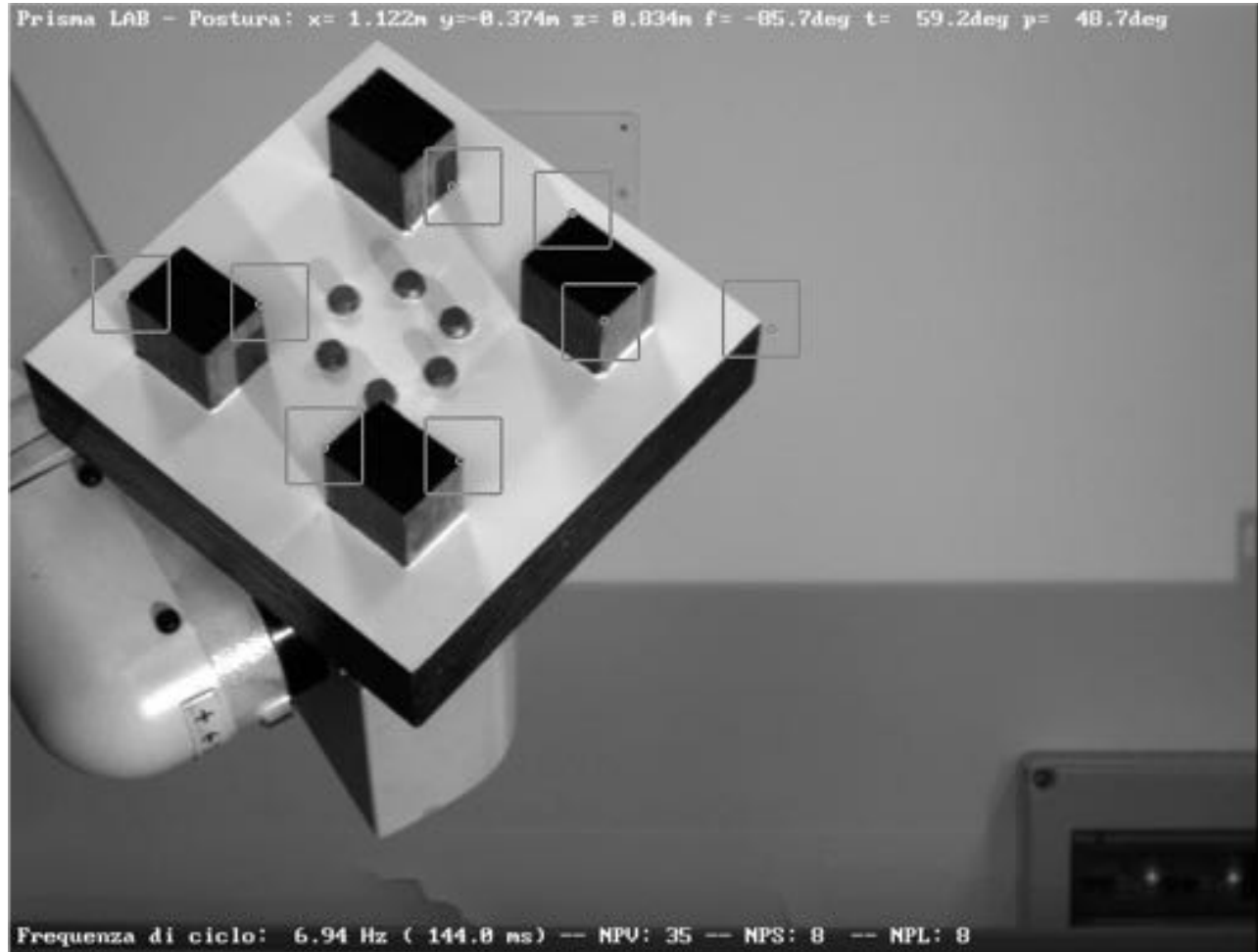
# Manipulators and vision systems

- CCD camera mounted on the robot for controlling the end-effector positioning (**eye-in-hand**)





# Visual tracking eye-to-hand

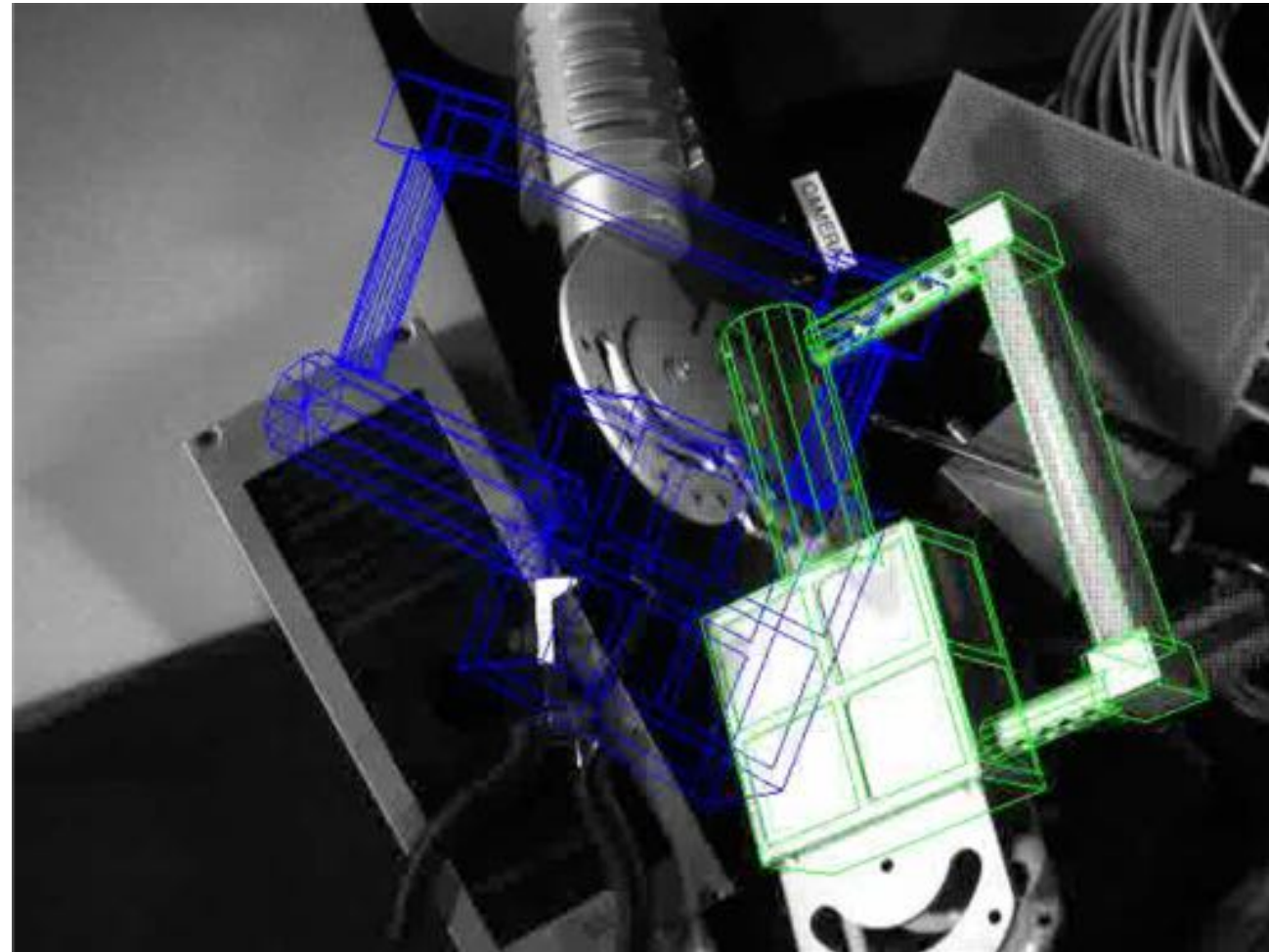


video

COMAU robot with position-based 6D tracking from external camera  
(DIS, Università di Napoli Federico II)



# Visual servoing eye-in-hand

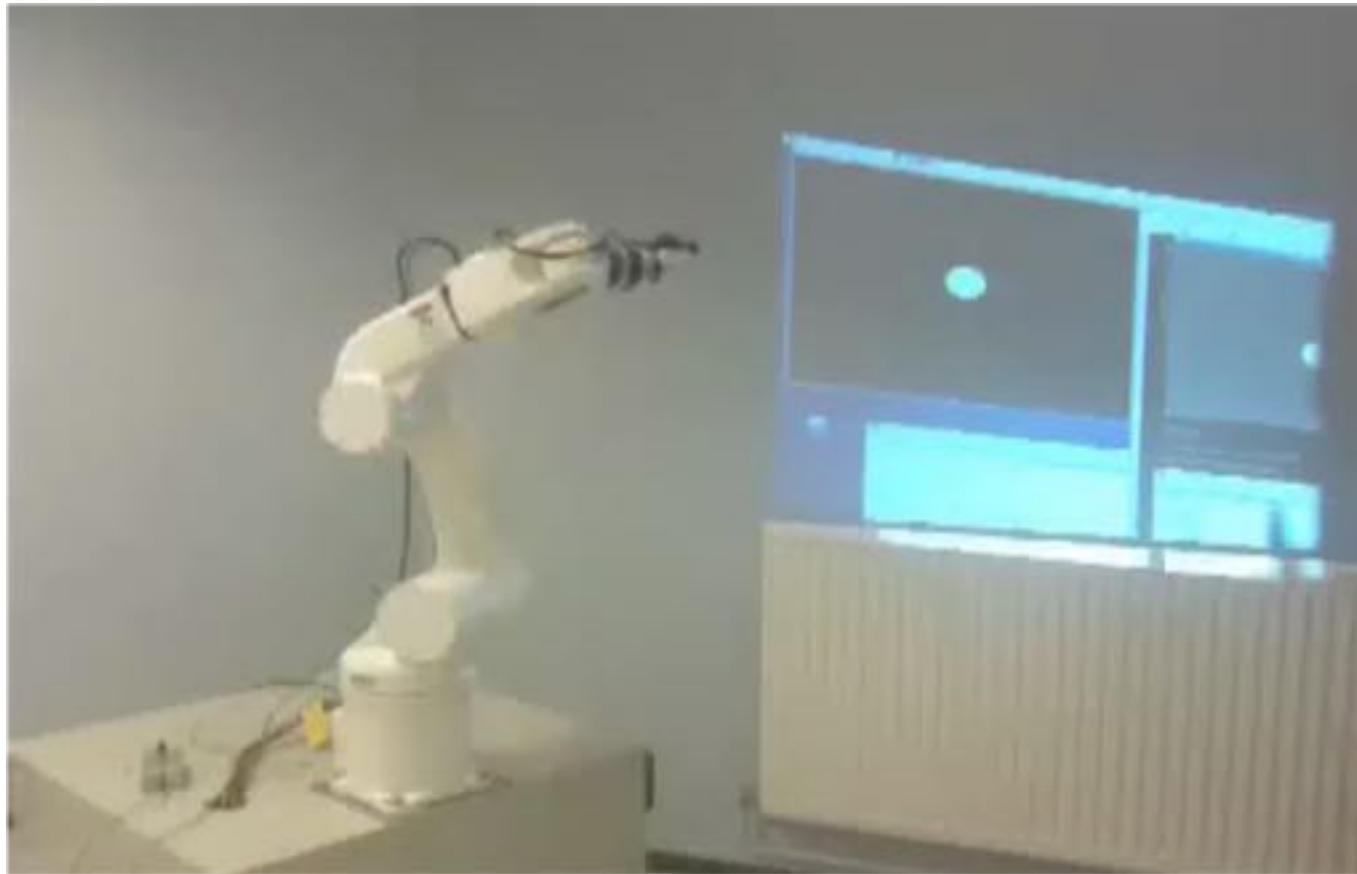


video

Image-based servoing with camera mounted on the robot end-effector  
(IRISA/INRIA, Rennes)



# Visual servoing and redundancy



[video](#)

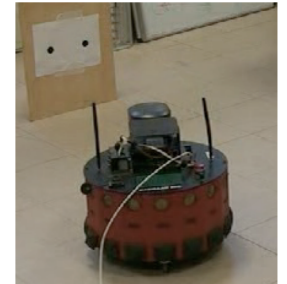
Visual servoing of a point feature ( $m=2$ ) with Adept Viper robot ( $n=6$ ): redundancy is used for avoiding joint range limits (IRISA/INRIA, Rennes)



# Visual servoing with mobile robot

video

pan/tilt (2 dof)  
web cam at 7Hz  
frame rate



Video attachment to ICRA'08 paper

Visual Servoing with Exploitation of Redundancy:  
An Experimental Study

A. De Luca

M. Ferri

G. Oriolo

P. Robuffo Giordano

Dipartimento di Informatica e Sistemistica  
Università di Roma "La Sapienza"

On-board image-based visual servoing with Magellan mobile robot  
(DIS Robotics Laboratory, IEEE ICRA'08)



# Combined visual/force assembly



KUKA LWR with eye-in-hand camera and F/T sensor  
(DLR, IEEE ICRA'07 demo in Roma)

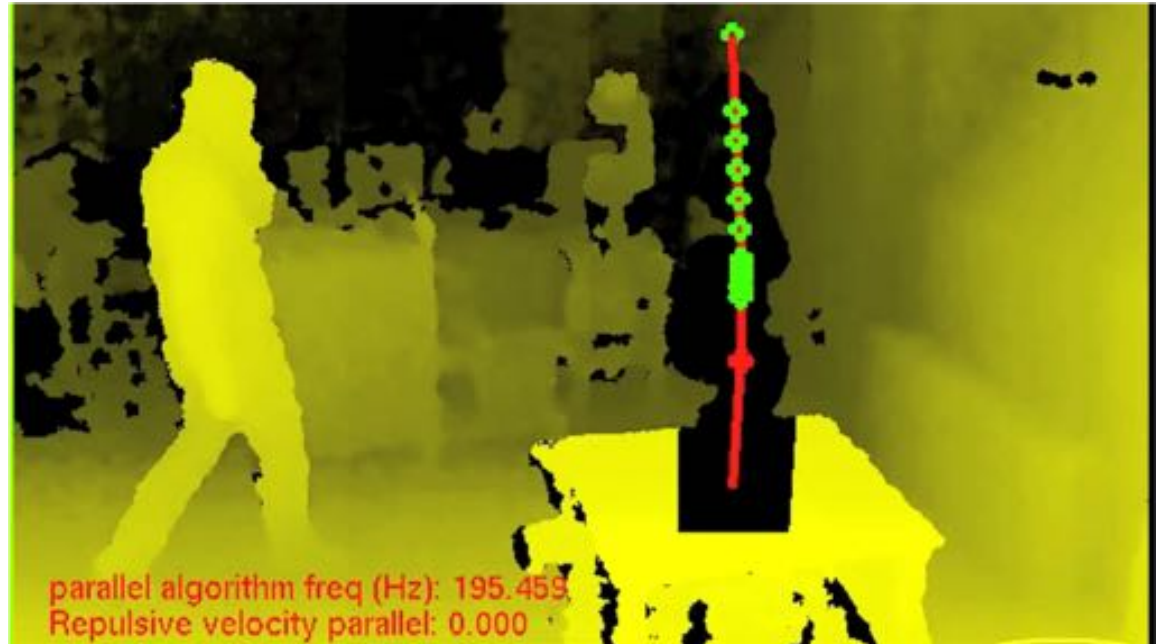
# On-line distance computation and human-robot coexistence



video



monitoring **left-** and **right-hand**  
distance to the robot (at same time)



several **control points** on robot **skeleton**  
used to compute distances and control motion

KUKA LWR with a Kinect monitoring its workspace  
(DIAG Robotics Laboratory, EU project SAPHARI, 2013)